Nonlocal electron-positron correlations in solids within the weighted density approximation

A. Rubaszek
W. Trzebiatowski Institute of Low Temperature and Structure Research, Polish Academy of Sciences, P.O. Box 937, 50-950 Wrocław 2, Poland

Z. Szotek* and W. M. Temmerman†
Daresbury Laboratory, Warrington, WA4 4AD, Cheshire, United Kingdom
(Received 7 January 1998; revised manuscript received 30 April 1998)

Nonlocal electron-positron correlation effects in solids are studied. The weighted density approximation (WDA) is applied to calculations of the nonlocal state-selective electron-positron correlation functions. The importance of state selectivity of the electron-positron enhancement factors is discussed. The calculated WDA electron-positron enhancement factors for the core electrons are compared with those obtained within the local-density approximation. Also, differences in the electron-positron enhancement factors due to the s, p, d, and f angular momentum channels of the electron charge density are studied. The influence of the electron-positron interaction on the positron density distribution in solids is discussed. The formalism is applied to *ab initio* calculations of positron lifetimes in a variety of metals and silicon. The influence of various approximations to the electron-positron interaction on the positron lifetimes is also presented. Moreover, we study how the core electrons as well as different angular momentum channels of the valence electron density contribute to the total positron annihilation rates and lifetimes. The results are compared to those calculated within the local-density approximation and the generalized gradient approximation. [S0163-1829(98)06037-8]

I. INTRODUCTION

Positrons are a sensitive probe of the electronic structure of solids.[1] The positron lifetime τ provides information on the electron-density distribution in the host material, thus yielding also useful information on defects in metals and semiconductors. The angular correlation of positron annihilation radiation (ACAR) spectra contain information on the electron momentum density and the shape of the Fermi surface. However, this information is distorted by the positron wave function and many-body electron-positron (e-p) correlation effects. Therefore, in the interpretation of the positron annihilation data, in terms of the electronic structure, knowledge of the e-p correlations is of vital importance.[1,2] Nevertheless, an incorporation of the exact e-p interaction effects in calculations of the positron lifetime and ACAR spectra in solids is very difficult.[3] The essential problem lies in the fact that the e-p correlation functions depend in general on both the initial electron state and positron position. In particular, calculations[4–10] show that the positron annihilation characteristics are very sensitive to the angular momentum decomposition of the electron wave function. This state selectivity of the e-p correlations has been well documented by ACAR spectra for simple metals,[11] and some transition-metal systems such as zinc[4] or vanadium.[12]

The position dependence of the e-p correlations cannot be neglected in studies of defects,[13,14] at a metal surface,[15,16] or for strongly localized electrons in the bulk, e.g., d and f electrons in transition metals or core electrons.[5,6,9,10,12,17] It has been a common practice in calculations of the positron annihilation characteristics to treat the position-dependent e-p interaction within the local-density approximation (LDA).[2,4–6,9,12–14,18–21] In this approximation, the e-p correlations are replaced by their analogues in a homogeneous electron gas with the local electron density $n(\mathbf{r}_p)$ at the positron position $\mathbf{r}_p$. This approximation is known to work well for systems with slowly varying electron densities, e.g., for valence electrons in simple metals. However, there exist several parametrizations of the jellium correlation functions,[2,22,23] and the LDA results are dependent on the choice of these parametrizations. In this paper, we compare the positron lifetimes calculated for four different parametrizations. Another important issue is the positron annihilation with the core electrons. Indeed, theoretical,[5–7,17–20] semiempirical,[8] and experimental[24] studies have shown that the core electron's contribution to the annihilation characteristics is non-negligible in comparison with the valence electron's contribution. However, for core electrons, due to strong variations of the density, the LDA is not expected to work very well. In fact, for the localized core electrons the LDA seems to overestimate the e-p correlation effects, and in particular, in the interstitial region. The same occurs for localized d and f electrons in transition metals, rare earths, and actinides. As a result, the LDA underestimates the positron lifetimes, as compared with the experimental data.[25] This discrepancy may be caused by nonlocal effects. A purpose of this paper is to study the influence of these nonlocal correlations, evaluated within the weighted density approximation, on the positron lifetimes in solids.

By nonlocality of the electron-positron correlations one usually means that the enhancement of the electron density at the positron position is dependent on the total electron density in the whole coordinate space of the system, or at least in the region defined by the range of the electron screening cloud surrounding the positron. This condition for nonlocality, expressed in terms of momenta, has been satisfied by the e-p scattering amplitudes obtained within the Bloch-modified ladder diagrams approximation to the zero-temperature e-p Green's function.[3] The approach has been successfully applied in calculations of the momentum densities for valence electrons in a number of metals. However, for the core electrons some modifications to this formalism would be needed.

Some form of nonlocality of the e-p interaction was introduced by Barbiellini *et al.*,[26,27] who evaluated the e-p contact density (screening charge density at the positron position) within the generalized gradient approximation (GGA) for the momentum densities and total annihilation rates. This approach, however, makes use of a parameter-dependent e-p correlation function and the adjustable parameter is fitted to the experimental data. The GGA has also been utilized by Alatalo *et al.*[17] in the calculation of the momentum densities and Doppler broadening of the annihilation radiation.

The weighted density approximation includes nonlocal effects through substituting the electron density $n(\mathbf{r}_p)$ in the LDA correlation function, by its weighted average $n^*(\mathbf{r}_p)$, where the distribution of the electron polarization cloud, surrounding the positron, provides the weighting factor. The WDA was first introduced by Gunnarsson *et al.*[28] for studying the nonlocal electron-electron correlations and exchange effects. The WDA can be interpreted as an *ab initio* generalization of the LDA for strongly inhomogeneous systems. When the electron density is slowly varying, the WDA reduces to the LDA. The former has been successfully applied to the problem of positron interaction with a metal surface,[15,16] leading to a much improved description of the positron screening at surfaces, as compared with the LDA.

In this paper we utilize the WDA to calculate the nonlocal e-p correlation functions in solids. We determine the e-p correlation potentials and study the influence of the e-p interaction on the positron density distribution. We evaluate the contributions of the core and valence electrons to the electron screening cloud around the positron. The valence electrons contribution is further decomposed into s, p, d, and f angular momentum channels. These nonlocal e-p effects are discussed in detail in the example of potassium (a simple metal with a large core size) and gold ($4d$-electron metal). Moreover, we study their influence on the positron lifetimes for a number of metals and silicon. In doing so, we concentrate on the effect of the nonlocality and state selectivity of the enhancement factors on the total annihilation rates $\lambda = 1/\tau$, and evaluate the importance of the contributions of s, p, d, f, and core electrons to the total annihilation rates. The positron lifetimes, calculated using various approximations for the e-p correlations in solids, are also compared with experimental data.[25]

The organization of the present paper is as follows. In Sec. II we elaborate on the formalism and give details of the calculations. The results are presented and discussed in Sec. III, and in Sec. IV we conclude the paper.

II. THEORY

The electronic structure of solids is usually calculated within the density-functional theory (DFT).[29] The electron charge density $n(\mathbf{r}_e)$, at the position $\mathbf{r}_e$ in the host material, is an important ingredient for the calculations of the positron lifetimes. It consists of a core, n_c, and valence, n_v, contribution. The valence contribution $n_v(\mathbf{r}_e)$ can be further decomposed into the angular momentum components $n_l(\mathbf{r}_e)$, of which we shall make use in the calculations of the e-p correlation functions. Consequently, throughout this paper, we shall use quantities with a subscript t, when considering specific contributions due to different types of electrons, and with no subscript, when the total quantities are of interest. Here t may stand for c (core), v (valence), s, p, d, and f electrons.

A. Enhancement factors and the weighted density approximation

When a positron enters a solid, it attracts the surrounding electrons, and for a positron at $\mathbf{r}_p$, a polarization cloud with the distribution $n(\mathbf{r}_e)[g(\mathbf{r}_e,\mathbf{r}_p,Q=1)-1]$ is formed at $\mathbf{r}_e$. Here $g(\mathbf{r}_e,\mathbf{r}_p,Q)$ is the correlation function of the fully interacting one-positron N-electron system. The variable $Q \in [0,1]$ is a scaling parameter, which has the meaning of an impurity charge.[15,22] The value $Q=1$ corresponds to the case where the e-p correlations are fully taken into account, and $Q=0$ refers to the independent-particle model (IPM) approximation.

The e-p enhancement factors $\gamma(\mathbf{r}_p)=g(\mathbf{r}_p,\mathbf{r}_p,1)$ for the total charge density, and $\gamma_t(\mathbf{r}_p)=g_t(\mathbf{r}_p,\mathbf{r}_p,1)$ for the partial charge densities, i.e., the state-dependent enhancement factors are defined as the ratios of the relevant perturbed and unperturbed electron densities at the positron position $\mathbf{r}_p$. These position-dependent enhancement factors, $\gamma_t(\mathbf{r}_p)$, have usually been evaluated within the LDA,[1,2,4–6,9,12–14,18–21] and approximated by $\gamma_t^h[n(\mathbf{r}_p)]$,[22] which are the corresponding quantities for the homogeneous electron gas of local electron density $n(\mathbf{r}_p)$ at the positron position $\mathbf{r}_p$.

In the present paper we generalize the LDA state- and position-dependent correlation functions to the nonlocal case, formulated within the WDA. In the nonlocal approach of the WDA,[15,16] the correlation functions are approximated by $g_t^{WDA}(\mathbf{r}_e,\mathbf{r}_p,Q)=g_t^h[|\mathbf{r}_e-\mathbf{r}_p|,n^*(\mathbf{r}_p),Q]$, where $n^*(\mathbf{r}_p)$ is an effective WDA density. The density $n^*(\mathbf{r}_p)$ is defined, for any positron position $\mathbf{r}_p$, as the solution of the charge neutrality condition that states that the electron charge, screening an impurity with the charge Q, is equal to $-Q$. In terms of the correlation functions this condition can be written as

$$\int d\mathbf{r}_e n(\mathbf{r}_e)\{g^h[|\mathbf{r}_e-\mathbf{r}_p|,n^*(\mathbf{r}_p),Q]-1\}=Q. \qquad (1)$$

Here we further generalize the above equation and define the effective electron densities, $n_t^*(\mathbf{r}_p)$, for every different type t (Ref. 28) (technical details of calculating the effective electron densities are given in the Appendix). This means that, for any t and $\mathbf{r}_p$, we seek the density

$$\tilde{n}_t(\mathbf{r}_p)=n(\mathbf{r}_p)+[n_t^*(\mathbf{r}_p)-n_t(\mathbf{r}_p)]$$

as the solution of the charge-neutrality equation

$$\int d\mathbf{r}_e n_t(\mathbf{r}_e)\{g_t^h[|\mathbf{r}_e-\mathbf{r}_p|,\tilde{n}_t(\mathbf{r}_p),Q]-1\} = Q\frac{\{g_t^h[0,n(\mathbf{r}_p),Q]-1\}n_t(\mathbf{r}_p)}{\Sigma_{t'}\{g_{t'}^h[0,n(\mathbf{r}_p),Q]-1\}n_{t'}(\mathbf{r}_p)}. \qquad (2)$$

The corresponding WDA correlation function for electrons of type t is approximated by its analogue in an electron gas of local density $\tilde{n}_t(\mathbf{r}_p)$.

Note that the solutions of Eq. (2) satisfy Eq. (1). If for a given type of electrons, t, the density $n_t(\mathbf{r}_e)$ is slowly varying, in the vicinity of the positron position $\mathbf{r}_p$, namely, when $n_t(\mathbf{r}_e)\cong n_t(\mathbf{r}_p)$, then the solution of Eq. (2) is $\tilde{n}_t(\mathbf{r}_p)=n(\mathbf{r}_p)$ $[n_t^*(\mathbf{r}_p)=n_t(\mathbf{r}_p)]$. The corresponding enhancement factor, $\gamma_t^{WDA}(\mathbf{r}_p)=\gamma_t^h[\tilde{n}_t(\mathbf{r}_p)]$, is close to $\gamma_t^{LDA}(\mathbf{r}_p)=\gamma_t^h[n(\mathbf{r}_p)]$, and therefore, for these electrons, the WDA reduces to the LDA. However, the LDA and WDA differ significantly, when the t dependence of the input enhancement factors of jellium is neglected, namely, when it is assumed that $\gamma_t^h(n_0)\equiv\gamma^h(n_0)$.[12,14,18–21,26] The resulting LDA enhancement factors become t independent, meaning that all types of electrons scatter on the positron at the same rate. In contrast, the corresponding WDA enhancement factors remain t selective, provided $\tilde{n}_t(\mathbf{r}_p)$ differs from $n(\mathbf{r}_p)$.

Another important point concerning the WDA is that, even though the density $n(\mathbf{r}_p)$ of the host material (as used in the LDA) is equal to the sum of partial densities $n_t(\mathbf{r}_p)$, the WDA total electron density $n^*(\mathbf{r}_p)=\tilde{n}(\mathbf{r}_p)$ cannot be expected to be equal to the sum of densities $n_t^*(\mathbf{r}_p)$. The only WDA quantity that is a direct sum of all contributions t is the density of the screening cloud at the positron position. The total density $n^*(\mathbf{r}_p)$ should rather be interpreted as a *weighted* sum of densities $n_t^*(\mathbf{r}_p)$, where the correlation functions are the weights. This means that

$$n(\mathbf{r}_p)\gamma^h[\tilde{n}(\mathbf{r}_p)]=\sum_t n_t(\mathbf{r}_p)\gamma_t^h[\tilde{n}_t(\mathbf{r}_p)],$$

where $\tilde{n}(\mathbf{r}_p)=n^*(\mathbf{r}_p)$.

The above relation between $\tilde{n}$ and $\tilde{n}_t$ (n^* and n_t^*) implies that if in some region of space a particular type of electron, t_0, dominates the total electron density of the host material, $n(\mathbf{r}_p)$, then in that region the shape of the WDA enhancement factor for the whole system, $\gamma^{WDA}(\mathbf{r}_p)$, should be close to $\gamma_{t_0}^{WDA}(\mathbf{r}_p)$.

B. Positron wave function and electron-positron correlation potential

The positron wave function $\psi_+(\mathbf{r}_p)$ is a solution of the Schrödinger equation

$$[-\tfrac{1}{2}\nabla^2-V_{ext}(\mathbf{r}_p)-V_H(\mathbf{r}_p)+V_{corr}(\mathbf{r}_p)]\psi_+(\mathbf{r}_p)=E_+\psi_+(\mathbf{r}_p),$$

with the energy E_+ being the positron bottom of the band. The positron potential consists of the external potential due to ions ($-V_{ext}$), the Hartree potential ($-V_H$), and e-p correlation (V_{corr}) potential.[7,13,14] The positron Hartree potential is equal to the electron Hartree potential, but has the opposite sign. The same holds for the external potential. The potential V_{corr}, describing the positron interaction with the electron screening cloud, is calculated according to the Feynmann's theorem[7,13–16,22,28,30]

$$V_{corr}(\mathbf{r}_p)=-\int_0^1 dQ\int d\mathbf{r}_e n(\mathbf{r}_e)\,\frac{g(\mathbf{r}_e,\mathbf{r}_p,Q)-1}{|\mathbf{r}_e-\mathbf{r}_p|}.$$

Obviously, for the IPM, $V_{corr}^{IPM}(\mathbf{r}_p)\equiv 0$. Within the LDA the e-p correlation potential is approximated by its homogeneous electron-gas counterpart, namely, $V_{corr}^{LDA}(\mathbf{r}_p)=V_{corr}^h[n(\mathbf{r}_p)]$, which has been parametrized as a function of the density n_0.[22] The WDA e-p correlation potential is given by the formula

$$V_{corr}^{WDA}(\mathbf{r}_p)=-\sum_t\int_0^1 dQ\int d\mathbf{r}_e n_t(\mathbf{r}_e)\times\frac{g_t^h[|\mathbf{r}_e-\mathbf{r}_p|,\tilde{n}_t(\mathbf{r}_p),Q]-1}{|\mathbf{r}_e-\mathbf{r}_p|}. \quad (3)$$

This differs from the GGA expression where correlation function is reduced to the contact quantities $g(\mathbf{r}_p,\mathbf{r}_p,1)$ only. Therefore, for a given screening charge distribution, the Feynmann theorem can be used to calculate the corresponding WDA e-p correlation potential.

C. Positron annihilation rates

The total annihilation rate λ is calculated according to the formula

$$\lambda=\pi r_0^2 c\sum_t\int|\psi_+(\mathbf{r}_p)|^2 n_t(\mathbf{r}_p)\gamma_t(\mathbf{r}_p)d\mathbf{r}_p, \quad (4)$$

where r_0 and c are the classical electron radius and velocity of light, respectively. The positron wave function $\psi_+(\mathbf{r}_p)$ refers to a thermalized positron in the Bloch state of $\mathbf{k}_+=\mathbf{0}$ and the lowest positron band.

A very important issue in the calculations of the positron lifetimes in solids is the core electron's contribution to the screening cloud surrounding the positron. There are a number of calculations in the literature that differ in their treatment of this problem.[5,14,18–21,26] A few different approaches can be identified. In the first one, both the valence and core electrons are considered to scatter on the positron at the same rate, and only the position dependence of the enhancement factors is considered. Namely, it is assumed that $\gamma_v(\mathbf{r}_p)=\gamma_c(\mathbf{r}_p)=\gamma(\mathbf{r}_p)$.[17–21,26] Using the LDA for these enhancement factors leads in general to an overestimation of the annihilation rates.[26] An improvement on these calculated rates could be obtained with the GGA (Ref. 26) position-dependent enhancement factors, leading also to a better agreement with experiment.[25]

In the second approach it is assumed that the core electrons are not perturbed by a positron, i.e., they do not participate in a formation of the screening cloud. Therefore, $\gamma_c\equiv 1$ and $\gamma_v=\gamma(n_v)$.[18,19] This way one obtains an annihilation rate that is smaller than the rate calculated in the first approach, thus giving better agreement with experiments.

Both of the above approaches have some obvious faults. They do not consider the state selectivity of the enhancement factors and are extremal in their treatment of the core electrons, while the likelihood is that the core electrons do contribute to the screening cloud, but not to the same degree as the valence electrons. This view is supported by the slow positron experiments,[24] as well as by some semiempirical studies,[8] which indicate that the IPM, used in the second approach, does not give justice to what happens in reality. Also, it seems obvious that it must be more difficult for the

core electrons to be scattered to states with energies greater than the Fermi energy E_F than it is for the valence electrons. Therefore, assuming equal probabilities for both core and valence electrons, as done in the first approach, does not seem fully justified either. These points have been carefully considered and taken into account by Daniuk *et al.*,[5,6] who have assumed that $1 \leqslant \gamma_c \leqslant \gamma_v$. Consequently, the core enhancement factor $\gamma_c(\mathbf{r}_p)$ has been approximated by the function $\epsilon[0,n(\mathbf{r}_p)]$, and $\gamma_v(\mathbf{r}_p)$ has been set to $\gamma^h[n(\mathbf{r}_p)] \cong \epsilon[0.64,n(\mathbf{r}_p)] \geqslant \epsilon[0,n(\mathbf{r}_p)]$. Here $\epsilon(E,n_0)$ is the Kahana-type energy-dependent e-p enhancement factor in an electron gas of the density n_0.[22,23] Since this approach is known to give a very good agreement between the calculated LDA and experimental annihilation rates[25] and the ACAR spectra,[4,6] in this paper we employ it within the WDA. This is equivalent to approximating $\gamma_t(\mathbf{r}_p)$ in Eq. (4) by $\gamma_t^{WDA}(\mathbf{r}_p) = \epsilon[E_t/E_F, \tilde{n}_t(\mathbf{r}_p)]$, where E_t is the energy of the center of mass of the electrons of type t.

D. Details of calculations

In the calculations of the positron annihilation characteristics both within the LDA and GGA, only the e-p enhancement factors of the homogeneous electron gas, namely, $\gamma^h(n_0)$ and $\gamma_t^h(n_0)$, are required. However, as already mentioned above, in the WDA one needs to evaluate $g^h(|\mathbf{r}_e - \mathbf{r}_p|, n_0, Q)$ in the whole coordinate space, and for all $Q \in [0,1]$. If the interaction parameter Q is equal to the impurity charge then, as follows from the Thomas-Fermi approximation, the correlation function $g^h(0,n_0,Q)$ can be replaced by $1+Q[\gamma^h(n_0)-1]$.[15] Consequently, the functions $g^h[|\mathbf{r}_e - \mathbf{r}_p|, n(\mathbf{r}_p), Q]$ and their t-selective variants have been approximated, respectively, by the following exponential expression:[15,16,22,31]

$$g_t^h[|\mathbf{r}_e-\mathbf{r}_p|, n(\mathbf{r}_p), Q] = 1 + Q\{\gamma_t^h[n(\mathbf{r}_p)]-1\} \times e^{-a_{LDA}[n(\mathbf{r}_p)]|\mathbf{r}_e-\mathbf{r}_p|}.$$

In this case, the function $a_{LDA}[n(\mathbf{r}_p)]$ is obtained directly from the charge neutrality condition [Eq. (1)], namely,

$$a_{LDA}^3[n(\mathbf{r}_p)] = 8\pi \sum_t n_t(\mathbf{r}_p)\{\gamma_t^h[n(\mathbf{r}_p)]-1\}.$$

The densities $\tilde{n}_t(\mathbf{r}_p)$ have been evaluated for all positron positions $\mathbf{r}_p$ and all channels t, using Eq. (2), which for the above exponential form of the correlation functions becomes

$$\{\gamma_t^h[\tilde{n}_t(\mathbf{r}_p)]-1\} \int n_t(\mathbf{r}_e) e^{-a[\tilde{n}_t(\mathbf{r}_p)]|\mathbf{r}_e-\mathbf{r}_p|} d\mathbf{r}_e = \{\gamma_t^h[n(\mathbf{r}_p)]-1\} n_t(\mathbf{r}_p) 8\pi / a_{LDA}^3[n(\mathbf{r}_p)], \quad (5)$$

with

$$a^3[\tilde{n}_t(\mathbf{r}_p)] = \frac{n_t^*(\mathbf{r}_p)\{\gamma_t^h[\tilde{n}_t(\mathbf{r}_p)]-1\}}{n_t(\mathbf{r}_p)\{\gamma_t^h[n(\mathbf{r}_p)]-1\}} a_{LDA}^3[n(\mathbf{r}_p)].$$

In the present calculations, the self-consistent electron densities, $n(\mathbf{r}_e)$ and $n_t(\mathbf{r}_e)$, have been obtained using the linear muffin-tin orbitals (LMTO) method in the atomic sphere approximation (ASA).[32] For the core electrons we have implemented the frozen core approximation. This does not seem to appreciably influence the nonlocal effects studied in the present paper. Indeed, the WDA effective density for the core electrons is much less dependent on the positron position than the core electron density in the host material. Therefore, small changes in the core electron density, due to core electron relaxation, are not expected to alter the WDA results.

The enhancement factors $\gamma_t^h(n_0)$ have been approximated as follows: $\gamma_c^h(n_0) = \epsilon(0,n_0)$,[5,6] $\gamma_v^h(n_0) = \gamma^h(n_0)$,[5,14,18–21,26] and $\gamma_l^h(n_0) = \epsilon(E_{\nu l}/E_F, n_0)$,[4,5,9] where $E_{\nu l}$ and E_F have been calculated with respect to the bottom of the valence band. The energies $E_{\nu l}$ are the angular momentum l-dependent linearization energies of the LMTO-ASA band structure method. Moreover, for $\gamma^h(n_0)$, apart from the Rubaszek and Stachowiak (RS) electron-gas enhancement factors,[23] we have also used a few different parametrizations[22] for comparison. They are Arponen and Pajanne's enhancement factors, parametrized by Barbiellini *et al.*[26] (AP), Kallio, Lantto, and Pietiläinen's enhancement factors, parametrized by Boroński and Nieminen[13] (BN), and Stachowiak's enhancement factors, parametrized by Stachowiak and Lach[22] (SL).

While calculating the WDA enhancement factors, special attention has been paid to the zeros of the densities n_t. For these few isolated points, $\mathbf{r}_p = \mathbf{r}_t^0$, at which $n_t(\mathbf{r}_p) = 0$, the right-hand side of Eq. (2) is equal to zero, while the left-hand side is always positive, except for the unphysical case when $g^h[|\mathbf{r}_e - \mathbf{r}_p|, \tilde{n}_t(\mathbf{r}_p), Q] = 1 + Q\,\delta(\mathbf{r}_e - \mathbf{r}_p)/\tilde{n}_t(\mathbf{r}_p)$. Therefore, at the nodes $\mathbf{r}_t^0$ of the density n_t, there exist no numerical solutions, $n_t^*(\mathbf{r}_t^0)$, of Eq. (2), and for $n_t(\mathbf{r}_t^0) = 0$, the values of $n_t^*(\mathbf{r}_t^0)$ have to be chosen arbitrarily. Nevertheless, the choice of the values of $n_t^*(\mathbf{r}_t^0)$ does not influence the partial and total annihilation rates [cf. Eq. (4)] for two reasons. One of them is that at $\mathbf{r}_p = \mathbf{r}_t^0$ the expression under the integral in Eq. (4) is equal to zero, for any value of $\tilde{n}_t(\mathbf{r}_p)$. The second reason is more general: the value of an integral of a finite function is independent of the values of this function on a finite set of isolated points (because the measure of this set is equal to zero).

III. RESULTS AND DISCUSSION

In this section we discuss in detail the nonlocal e-p correlation effects for potassium and gold. In what follows we consider separately the core and valence electrons, the latter also decomposed into different angular momentum channels. Moreover, we discuss the e-p correlation potentials and positron distributions, as obtained in the different approximations employed. We also study the importance of the nonlocal effects for the calculation of the total and partial positron annihilation rates. For this we have calculated the latter for a variety of metals and silicon, using three different approximations for the positron wave function and e-p correlations. Specifically, we have calculated the partial annihilation rates within the IPM, LDA, and WDA. While calculating the positron wave functions, we have used the same approximations for the positron correlation potential V_{corr}, occurring in the positron Schrödinger equation. Additionally, as mentioned

TABLE I. The core electrons contribution to the positron annihilation rates, as calculated according to Eq. (4), using the RS parametrization of $\epsilon(0,n_0)$. Numbers in columns (2), (3), and (6) correspond, respectively, to three different approximations used for the e-p correlation potential when calculating the positron wave function, namely, V_{corr}^{IPM}, V_{corr}^{LDA}, and V_{corr}^{WDA}. The superscript of λ specifies the approximation used for the e-p enhancement factors $\gamma_c(\mathbf{r})$, namely, IPM, LDA, and WDA. Also shown are the quantities $r_c^{LDA,WDA}$, describing relative changes in λ_c^{IPM} due to the shape of the positron distribution, and the average enhancement factors $\Gamma_c^{LDA(WDA)}$.

	ψ_+^{IPM}		ψ_+^{LDA}			ψ_+^{WDA}	
(1) Element	(2) λ_c^{IPM}	(3) λ_c^{LDA}	(4) $r_c^{LDA}(\%)$	(5) Γ_c^{LDA}	(6) λ_c^{WDA}	(7) $r_c^{WDA}(\%)$	(8) Γ_c^{WDA}
Alkali metals							
Li	0.1422	0.4259	13	2.66	0.5545	44	2.70
Na	0.1847	0.6236	21	2.78	0.5065	36	2.01
K	0.1311	0.6548	21	4.11	0.4202	18	2.78
Rb	0.1215	0.6898	21	4.68	0.3164	7	2.45
Cs	0.1064	0.7091	20	5.53	0.3426	3	3.13
Polyvalent metals							
Ca	0.032	0.096	19	2.53	0.091	31	2.17
Al	0.240	0.529	8	1.76	0.502	20	1.75
$3d$ transition metals							
V	0.832	1.867	6	2.11	1.625	10	1.77
Cr	0.929	1.964	6	1.99	1.753	11	1.71
Mn	0.780	1.616	7	1.94	1.471	13	1.67
Fe	0.741	1.490	8	1.87	1.382	14	1.63
Ni	0.662	1.265	8	1.76	1.212	17	1.56
Cu	0.515	0.978	10	1.73	0.950	20	1.54
$4d$ transition metals							
Nb	0.789	1.899	6	2.30	1.497	6	1.73
Mo	0.891	2.007	5	2.15	1.637	6	1.73
Pd	0.605	1.252	8	1.91	1.111	13	1.63
Ag	0.412	0.860	11	1.88	0.773	17	1.61
$5d$ transition metals							
Pt	0.617	1.234	8	1.86	1.062	11	1.55
Au	0.447	0.902	10	1.84	0.864	15	1.68
Semiconductors							
Si	0.060	0.142	27	1.82	0.160	48	1.80

before, for the input e-p enhancement factors in jellium, $\gamma_t^h(n_0)$, we have used four different parametrizations. [13,22,23,26] The results are summarized in Tables I–VI, with the values of λ in units of 10^9 s^{-1} and positron lifetimes in picoseconds.

A. Positron interaction with core electrons

In Fig. 1 we show the radial distributions of the normal and effective core electron densities, $4\pi r^2 n_c(\mathbf{r})$ and $4\pi r^2 n_c^*(\mathbf{r})$, respectively, both for potassium and gold, in the state-selective and state-independent modes as concerns the input e-p correlation functions of jellium. In this figure the corresponding enhancement factors, $\gamma_c^{LDA}(\mathbf{r})$ and $\gamma_c^{WDA}(\mathbf{r})$, are also presented. With respect to the nonlocal effects of the state-selective quantities, note that the densities $n_c^*(\mathbf{r})$ do not vary with $|\mathbf{r}|$ as much as the densities $n_c(\mathbf{r})$. The strong oscillations, observed in $n_c(\mathbf{r})$ close to the nuclei, are not present in $n_c^*(\mathbf{r})$. At small distances away from the center of the ASA sphere (for $r \leqslant 0.5$ a.u.), where the core electron densities are very high, the effective WDA densities $n_c^*(\mathbf{r})$ are appreciably smaller than $n_c(\mathbf{r})$. This means that in this region the positron is screened more by the core electrons than it would follow from the LDA. Indeed, the WDA enhancement factors $\gamma_c^{WDA}(\mathbf{r})$ are higher than the corresponding LDA enhancement factors $\gamma_c^{LDA}(\mathbf{r})$. Of course, since the total electron density $n(\mathbf{r})$ is rather high for $r \leqslant 0.5$ a.u., the corresponding WDA and LDA core enhancement factors are close to unity. Although the effective WDA electron densities $n_c^*(\mathbf{r})$ differ strongly from $n_c(\mathbf{r})$, this does not seem to substantially influence the e-p enhancement factors $\gamma_c^{WDA}(\mathbf{r} \cong \mathbf{0})$, which are only slightly higher than $\gamma_c^{LDA}(\mathbf{r})$. When the positron distance from the nuclei increases, the density

TABLE II. The state-selective average enhancement factors $\Gamma_t^{LDA(WDA)}=\lambda_t^{LDA(WDA)}/\lambda_t^{IPM}$ and the relative quantities $r_t^{LDA(WDA)}$, describing relative changes in λ_t^{IPM} due to the shape of the positron distribution. The partial annihilation rates λ_t^{LDA} and λ_t^{WDA} are given in Table IV. Numbers in columns (2)–(7) and (8)–(13) correspond, respectively, to the positron wave function determined from the Schrödinger equation with V_{corr}^{LDA} and V_{corr}^{WDA}. The subscripts of Γ define the type of electrons, while the superscripts specify the approximation used for the e-p enhancement factors $\gamma_t(\mathbf{r})$, namely, LDA and WDA.

	ψ_+^{LDA}						ψ_+^{WDA}					
(1) Element	(2) $r_s^{LDA}(\%)$	(3) $r_p^{LDA}(\%)$	(4) $r_{d+f}^{LDA}(\%)$	(5) Γ_s^{LDA}	(6) Γ_p^{LDA}	(7) Γ_{d+f}^{LDA}	(8) $r_s^{WDA}(\%)$	(9) $r_p^{WDA}(\%)$	(10) $r_{d+f}^{WDA}(\%)$	(11) Γ_s^{WDA}	(12) Γ_p^{WDA}	(13) Γ_{d+f}^{WDA}
Alkali metals												
Li	−0.1	−0.1		8.20	8.17		−0.5	−0.8		8.32	9.00	
Na	−0.1	−0.8		11.55	12.91		−0.3	−0.8		11.56	13.41	
K	−0.3	−1.3	−0.9	16.40	18.53	19.07	−0.3	−0.6	−0.3	16.64	19.43	19.31
Rb	−0.3	−1.4	−0.8	18.44	21.16	21.63	−0.2	0.3	0.2	18.79	22.35	22.05
Cs	−0.4	−1.6	−0.5	21.77	25.10	25.26	−0.1	1.6	0.3	22.35	26.55	25.99
Polyvalent metals												
Ca	0.0	−0.9	4.7	7.39	8.37	6.14	0.0	−1.4	7.9	7.34	8.78	4.48
Al	0.3	0.0	−0.3	4.01	4.33	4.55	0.7	0.0	−0.6	4.16	4.44	4.69
$3d$ transition metals												
V	−0.4	−0.7	1.3	3.55	3.94	3.58	−0.6	−0.1	2.0	3.58	4.03	3.25
Cr	−0.4	−0.6	1.6	3.25	3.57	3.16	−0.6	−0.9	2.6	3.28	3.65	2.84
Mn	−0.3	−0.6	2.1	3.33	3.67	3.20	−0.5	−1.0	3.7	3.34	3.75	2.79
Fe	−0.3	−0.6	2.5	3.28	3.61	3.11	−0.5	−1.0	4.6	3.31	3.69	2.66
Ni	−0.1	−0.5	3.1	3.25	3.57	3.00	−0.3	−1.0	6.2	3.26	3.64	2.52
Cu	0.0	−0.5	3.9	3.41	3.73	2.93	−0.1	−1.0	7.7	3.41	3.81	2.40
$4d$ transition metals												
Nb	−0.4	−0.7	0.7	3.60	4.00	3.65	−0.4	−0.6	0.7	3.63	4.08	3.47
Mo	−0.4	−0.7	0.9	3.23	3.55	3.18	−0.4	−0.6	1.0	3.26	3.62	3.00
Pd	−0.2	−0.7	2.8	3.34	3.67	3.00	−0.4	−1.1	4.4	3.36	3.75	2.62
Ag	−0.1	−0.7	4.1	3.69	4.04	2.83	−0.1	−1.1	6.3	3.68	4.14	2.39
$5d$ transition metals												
Pt	−0.1	−0.6	2.0	3.08	3.41	2.97	−0.1	−0.9	2.8	3.08	3.49	2.69
Au	0.1	−0.7	3.0	3.31	3.70	2.98	0.2	−1.0	4.5	3.30	3.78	2.62
Semiconductors												
Si	5.2	7.2	3.3	4.93	4.59	5.33	7.8	10.7	5.1	4.28	4.27	5.34

$n_c^*(\mathbf{r})$ becomes higher than $n_c(\mathbf{r})$, both in potassium and gold. As a result, $\gamma_c^{WDA}(\mathbf{r})$ in potassium can be as much as three times smaller than $\gamma_c^{LDA}(\mathbf{r})$, and about 75% smaller in gold. This is consistent with expectations, and has clear physical meaning: For a positron located far from the nuclei, it is much easier to attract valence electrons than tightly bound core electrons. Therefore, valence electrons dominate in the electron polarization cloud, while the core part of the screening cloud, loosing its spherical symmetry of the LDA, is shifted away from the positron towards the nuclei. Also, it is interesting that the shape of the WDA core enhancement factors is similar to the GGA result for the *total* electron density.[26]

In general, the WDA smoothes out the variation of the correlation functions $\gamma_c^{WDA}(\mathbf{r})$, in comparison with the LDA. The relative differences between $\gamma_c^{WDA}(\mathbf{r})$ and $\gamma_c^{LDA}(\mathbf{r})$ are larger in potassium than in gold. This seems to be mainly due to rather larger core size in potassium and lower electron densities, as compared to gold.

Let us now concentrate on the influence of the state selectivity of the input e-p correlation functions of jellium on the resulting LDA and WDA enhancement factors. For that in Fig. 1 we compare the state-selective enhancement factors with their state-independent counterparts, calculated assuming $\gamma_c^{LDA}(\mathbf{r})=\gamma^h[n(\mathbf{r})]$ (Refs. 18–21,26) and $\gamma_c^{WDA}(\mathbf{r})=\gamma^h[\tilde{n}_c(\mathbf{r})]$. Note, that for a positron close to the nuclei, the effective core densities, calculated in the state-independent approach, are higher than those obtained within the state-selective approach. This effect is most pronounced close to the maxima of the $4\pi r^2 n_c^*(\mathbf{r})$ distributions. At larger distances from the nuclei, the densities $n_c^*(\mathbf{r})$, obtained both within the state-selective and state-independent modes, are very close to each other. However, in this region, one observes large differences in the corresponding e-p enhancement factors. Both the LDA and WDA enhancement factors, resulting from the state-independent approach, are higher than the corresponding quantities calculated using $\epsilon[0,n(\mathbf{r})]$ and $\epsilon[0,\tilde{n}_c(\mathbf{r})]$, for the LDA and WDA, respectively. Also,

TABLE III. The total valence electrons contribution to the positron annihilation rates calculated according to Eq. (4), using the BN parametrization of $\gamma^h(n_0)$. Numbers in columns (2), (3), and (6) correspond, respectively, to the positron wave function determined from the Schrödinger equation with V_{corr}^{IPM}, V_{corr}^{LDA}, and V_{corr}^{WDA}. The superscripts of λ specify the approximation used for the e-p enhancement factors $\gamma_v(\mathbf{r})$, namely, LDA and WDA. Also shown are the quantities $r_v^{LDA(WDA)}$ describing relative changes in λ_v^{IPM} due to the positron distribution and the average enhancement factors $\Gamma_v^{LDA(WDA)}$ defined as $\Gamma_v^{LDA(WDA)} = \lambda_v^{LDA(WDA)}/\lambda_v^{IPM}$.

	ψ_+^{IPM}		ψ_+^{LDA}			ψ_+^{WDA}	
(1) Element	(2) λ_v^{IPM}	(3) λ_v^{LDA}	(4) $r_v^{LDA}(\%)$	(5) Γ_v^{LDA}	(6) λ_v^{WDA}	(7) $r_v^{WDA}(\%)$	(8) Γ_v^{WDA}
			Alkali metals				
Li	0.351	2.848	−0.14	8.11	2.891	−0.14	8.28
Na	0.194	2.322	−0.36	11.96	2.379	−0.36	12.33
K	0.110	1.955	−0.64	17.77	2.090	−0.27	19.0
Rb	0.090	1.836	−0.66	20.42	1.978	0.01	21.98
Cs	0.071	1.712	−0.74	24.46	1.873	0.33	26.38
			Polyvalent metals				
Ca	0.566	3.546	3.80	6.04	2.490	8.54	4.05
Al	1.362	5.499	−0.07	4.04	5.519	−0.07	4.28
			$3d$ transition metals				
V	1.932	6.579	0.62	3.38	6.065	1.04	3.11
Cr	2.452	7.791	0.73	3.15	7.094	1.39	2.85
Mn	2.471	7.940	1.09	3.16	6.990	2.19	2.77
Fe	2.641	8.303	1.40	3.11	7.237	3.29	2.65
Ni	2.946	9.006	1.90	3.09	7.670	4.72	2.49
Cu	2.660	8.398	2.37	3.08	6.960	5.98	2.47
			$4d$ transition metals				
Nb	1.771	6.148	0.34	3.46	5.892	0.51	3.31
Mo	2.331	7.473	0.43	3.19	7.226	0.56	3.08
Pd	2.663	8.370	1.95	3.08	7.325	3.83	2.62
Ag	2.198	7.372	2.82	3.26	6.204	5.73	2.67
			$5d$ transition metals				
Pt	3.049	9.279	0.34	3.0	8.386	2.39	2.69
Au	2.620	8.358	2.06	3.13	7.328	3.82	2.69
			Semiconductors				
Si	0.935	4.583	6.04	4.52	4.465	7.80	4.43

the effect of nonlocality of the e-p core enhancement factors is similar for both the state-selective and state-independent enhancement factors. The differences in the shape of $\gamma_c^{WDA}(\mathbf{r})$ vs $\gamma_c^{LDA}(\mathbf{r})$ follow nearly the same pattern in both cases.

B. Positron screening by valence electrons

In this subsection we concentrate on the nonlocal effects affecting the valence electrons in potassium and gold. We discuss in detail the effects for all the valence electrons and their decomposition into different angular momentum channels l. The results of relevance for this subsection are summarized in Figs. 2 and 3, where we present the WDA and LDA enhancement factors for valence electrons, respectively, in potassium and gold. The total quantities are further decomposed into the s, p, d (and f in gold) angular momentum channels. In all calculations of this subsection, the state-selective mode of the input jellium e-p correlation functions has been used.

Before discussing details of the corresponding enhancement factors, a few remarks are due. The contribution of a given angular momentum channel l to the WDA electron screening cloud, surrounding a positron located at the position $\mathbf{r}$, namely,

$$\Delta n_l^{WDA}(\mathbf{r}_e,\mathbf{r}) = n_l(\mathbf{r}_e)\{\gamma_l^h[\tilde{n}_l(\mathbf{r})]-1\}e^{-a[\tilde{n}_l(\mathbf{r})]|\mathbf{r}_e-\mathbf{r}|},$$

is rather nonspherical [due to the $\mathbf{r}_e$ dependence of $n_l(\mathbf{r}_e)$], extending strongly towards regions in space where the electrons of this angular momentum channel are to be found with the highest probability. The corresponding LDA screening charge is spherically symmetric, and can be described by the local jellium formula

TABLE IV. The contributions of the valence electrons, decomposed into different angular momentum channels, to the positron annihilation rates calculated according to Eq. (4) using the RS parametrization of $\gamma^h(n_0)$.

		ψ_+^{LDA}			ψ_+^{WDA}	
(1) Element	(2) λ_s^{LDA}	(3) λ_p^{LDA}	(4) λ_{d+f}^{LDA}	(5) λ_s^{WDA}	(6) λ_p^{WDA}	(7) λ_{d+f}^{WDA}
			Alkali metals			
Li	1.453	1.423		1.468	1.561	
Na	1.352	0.987		1.352	1.020	
K	1.081	0.658	0.155	1.097	0.694	0.156
Rb	1.030	0.550	0.174	1.051	0.592	0.179
Cs	0.957	0.431	0.227	0.984	0.468	0.234
			Polyvalent metals			
Ca	0.767	0.716	2.456	0.761	0.731	2.501
Al	1.285	3.227	1.160	1.337	3.313	1.191
			$3d$ transition metals			
V	1.317	1.717	4.071	1.325	1.751	3.724
Cr	1.371	2.012	4.697	1.378	2.051	4.260
Mn	1.427	2.008	4.871	1.430	2.046	4.317
Fe	1.430	2.010	5.253	1.434	2.045	4.587
Ni	1.534	1.957	5.951	1.535	1.984	5.149
Cu	1.558	1.929	5.120	1.555	1.958	4.358
			$4d$ transition metals			
Nb	1.071	1.152	4.360	1.081	1.176	4.140
Mo	1.107	1.467	5.035	1.115	1.496	4.757
Pd	1.123	1.343	6.045	1.126	1.367	5.361
Ag	1.162	1.339	4.755	1.160	1.366	4.113
			$5d$ transition metals			
Pt	1.220	1.620	6.585	1.221	1.651	6.013
Au	1.203	1.468	5.704	1.199	1.496	5.097
			Semiconductors			
Si	1.786	2.394	0.573	1.589	2.296	0.583

$$\Delta n_l^{LDA}(\mathbf{r}_e,\mathbf{r}) = n_l(\mathbf{r})\{\gamma_l^h[n_l(\mathbf{r})]-1\}e^{-a[n_l(\mathbf{r})]|\mathbf{r}_e-\mathbf{r}|}.$$

Note that the LDA and WDA correlation functions are spherically symmetric around the positron position and have the same form, however, with $\tilde{n}_l(\mathbf{r})$ being replaced by $n(\mathbf{r})$ in the LDA formula. The main reason for the asymmetry of the WDA screening charge is that the electron density $n_l(\mathbf{r}_e)$, occurring in the WDA formula, depends on the electron position $\mathbf{r}_e$. In contrast, the electron density $n_l(\mathbf{r})$, occurring in the LDA formula, is local, i.e., dependent only on the positron position, $\mathbf{r}$. As a consequence, in those regions of space towards which the WDA cloud extends, the corresponding WDA enhancement factors, $\gamma_l^{WDA}(\mathbf{r})$, are expected to be larger than their LDA counterparts. Moreover, if the contribution, $n_l(\mathbf{r})$, of a particular angular momentum channel, to the total electron density, $n(\mathbf{r})$, is nearly negligible in any region of space, then, in that region of space, the relevant WDA enhancement factors should be much the same as the LDA enhancement factors. Also, for nearly free electrons the LDA and WDA enhancement factors are expected to be very similar.

The first thing to note about Fig. 2, where the results for potassium are shown, is that the WDA and LDA valence electrons enhancement factors are not very different from one another. Since, in the vicinity of the nuclei the core electron density dominates in $n(\mathbf{r})$, therefore the corresponding WDA enhancement factors are very close to the LDA result. Further away from the center of the ASA sphere, moving towards its boundary, the nonlocality of the e-p correlation functions seems to influence differently different angular momentum channels of the valence electrons. Regarding the LDA enhancement factors for s, p, and d electrons, they are very similar in shape, and the differences between $\gamma_l^{LDA}(\mathbf{r})$'s for various l's are only due to the differences between the corresponding center-of-mass energies, $E_{\nu l}$. This is not the case for the WDA, for the s, p, and d electrons. As seen in panel (a), in the vicinity of the ASA sphere boundary (for $r>4.5$ a.u.) the WDA enhancement factor $\gamma_s^{WDA}(\mathbf{r})$ is a little smaller than the corresponding LDA enhancement factor. This follows from the fact that in this region the s-electron density, $n_s(\mathbf{r})$, decreases slightly, and the corresponding (almost constant) WDA effective density is

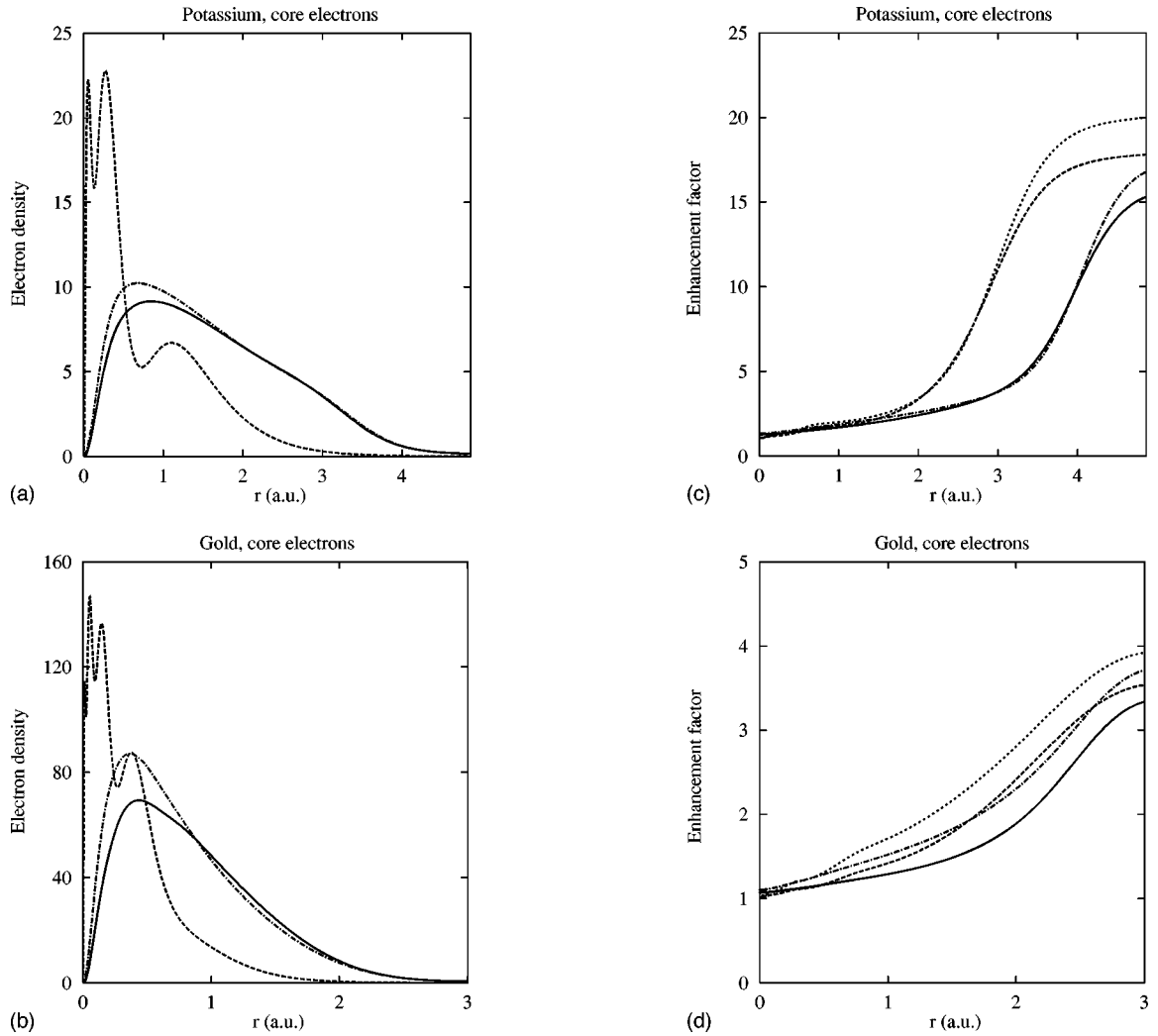

FIG. 1. Effective (WDA) and normal core electron densities multiplied by $4\pi r^2$, plotted as functions of r, for potassium (a) and gold (b). The solid curves correspond to the WDA result with the state-selective correlation functions, the dash-dotted curves refer to the WDA calculation with the non-state-selective correlation functions, and the dashed curves represent the normal electron densities. In parts (c) and (d) the corresponding results for the enhancement factors are shown. Potassium results are given in part (c) and the calculations for gold are shown in part (d). As in parts (a) and (b), the solid curves correspond to the WDA state selective enhancement factors, the dash-dotted curves refer to the WDA non-state-selective enhancement factors, the dashed curves are the LDA result for the state-selective enhancement factors, and the dotted curves are the result of the LDA with non-state-selective enhancement factors.

larger than $n_s(\mathbf{r})$. For a similar reason, the enhancement factor $\gamma_s^{WDA}(\mathbf{r})$ is larger than its LDA counterpart for 3 a.u. $<r<$4.5 a.u. In contrast to the s electrons, the WDA e-p enhancement factors for the p electrons are larger than $\gamma_p^{LDA}(\mathbf{r})$ if a positron is close to the ASA sphere boundary (for $r>4$ a.u.). This is because $n_p(\mathbf{r})$ increases slowly towards the ASA sphere boundary, reaching its highest value in this region, with $n_p^*(\mathbf{r})\leqslant n_p(\mathbf{r})$. When a positron is in the vicinity of the ASA sphere boundary it attracts more p electrons than it is predicted by the LDA. The d-electron enhancement factor is very LDA-like. The reason is that the d-electron density, $n_d(\mathbf{r})$, is a slowly varying function and its contribution to $n(\mathbf{r})$ is almost negligible. The enhancement factors due to the total number of valence electrons, $\gamma_v^{WDA}(\mathbf{r})$, reflect the above features of $\gamma_l^{WDA}(\mathbf{r})$ for the s, p, and d electrons. Note that the value of $\gamma_v^{WDA}(\mathbf{r})$ is intermediate in magnitude with respect to the values of $\gamma_s^{WDA}(\mathbf{r})$ and $\gamma_p^{WDA}(\mathbf{r})$, with d electrons hardly contributing to the positron screening. The valence part of the electron polarization cloud is slightly shifted towards the ASA sphere boundary, and therefore, for $r>3$ a.u., the resulting e-p enhancement factor, $\gamma_v^{WDA}(\mathbf{r})$, is a little higher than $\gamma_v^{LDA}(\mathbf{r})$. One can see that in potassium the nonlocal effects are of not much significance for the part of the screening cloud due to valence electrons. Relatively small differences between the LDA and WDA enhancement factors are observed mainly close to the ASA sphere boundary. In this respect, the present calculation differs significantly from the GGA approach.[26] The GGA enhancement factors are the same for the core and valence electrons. Due to a strong variation of $n_c(\mathbf{r})$ and a rather large core size of potassium, $\gamma^{GGA}(\mathbf{r})$ for the valence electrons is expected to differ substantially from $\gamma_v^{LDA}(\mathbf{r})$, which is clearly not the case for the WDA result.

In Fig. 3 we present the e-p enhancement factors for the valence electrons in gold. First, we concentrate on the WDA and LDA enhancement factors for s and p electrons. In this

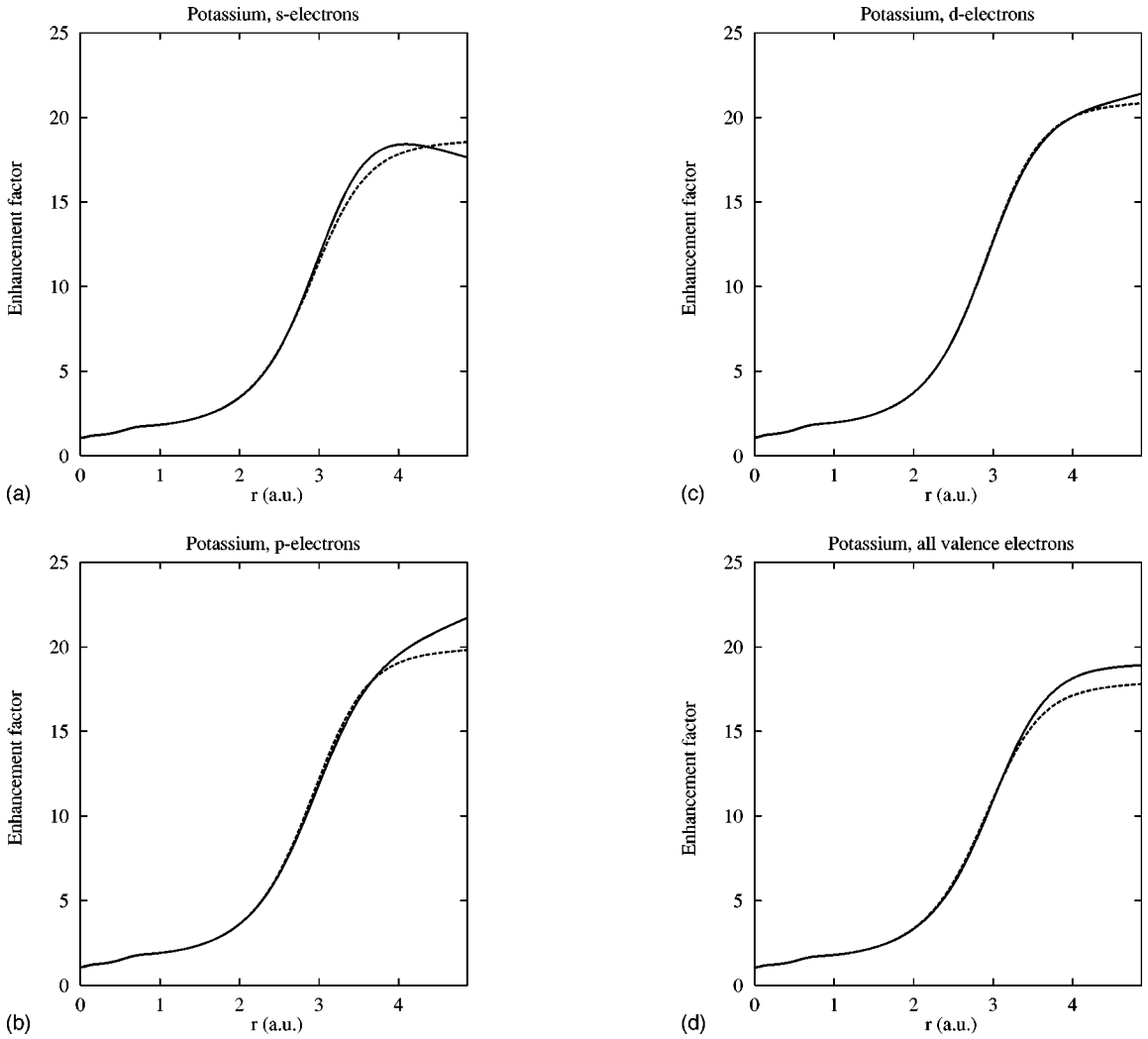

FIG. 2. Enhancement factors for potassium, plotted as functions of r, for the s-valence electrons (a), p-valence electrons (b), d-valence electrons (c), and the total number of valence electrons (d). The solid curves represent the WDA results and the dashed curves refer to the LDA calculation.

case the nonlocal effects are similar to potassium, although the observed differences between the LDA and WDA enhancement factors are even less pronounced than in potassium. Namely, in gold the WDA s and p enhancement factors are much more LDA-like. This result is mainly due to the higher total electron density in gold as compared to potassium. The essential differences between potassium and gold can be seen in the positron screening by d electrons. In gold, d electrons are strongly localized in the region of the intermediate $|\mathbf{r}|$'s, between the center and boundary of the ASA sphere. The d electron's density $n_d(\mathbf{r})$ is a strongly varying function, while the effective d-electron's density $n_d^*(\mathbf{r})$ is almost constant for $r>1$ a.u., and for 1 a.u.$<r<2$ a.u., the WDA effective density is considerably smaller than $n_d(\mathbf{r})$. As a consequence, the positron located in the region of the ASA sphere, preferred by d electrons, attracts more d electrons than it would follow from the LDA. Moreover, for 1 a.u.$<r<2$ a.u., the WDA enhancement factor is larger than the LDA enhancement factor. In the vicinity of the ASA sphere boundary ($r>2$ a.u.), the positron becomes detached from the d-electron part of the screening cloud. In this region, it is screened mainly by the delocalized s and p electrons, while the d-electron part of the polarization cloud is shifted towards the intermediate $|\mathbf{r}|$'s. As a result, the WDA d-electron enhancement factor is almost constant for $r>2$ a.u., and considerably smaller than the LDA enhancement factor. The f electrons density in gold is very small and therefore the corresponding WDA enhancement factors, $\gamma_f^{WDA}(\mathbf{r})$, are very LDA-like. The enhancement factors due to the total number of valence electrons, $\gamma_v^{WDA}(\mathbf{r})$, have a predominantly d character, because the d electron's density dominates in the total density of the valence electrons. For the intermediate $|\mathbf{r}|$'s, between the center and the boundary of the ASA sphere, the WDA enhancement factor is larger than the LDA enhancement factor, while close to the ASA sphere boundary, $\gamma_v^{WDA}(\mathbf{r})$ is appreciably smaller than $\gamma_v^{LDA}(\mathbf{r})$. This implies that the valence part of the electron screening cloud, losing the spherical symmetry of the LDA, is localized in the region of space preferred by d electrons (high valence electron density).

Concerning the ASA used in the present calculations, it affects the LDA enhancement factors much more than it is the case for the corresponding WDA quantities. The reason is that the LDA correlation functions directly reflect the elec-

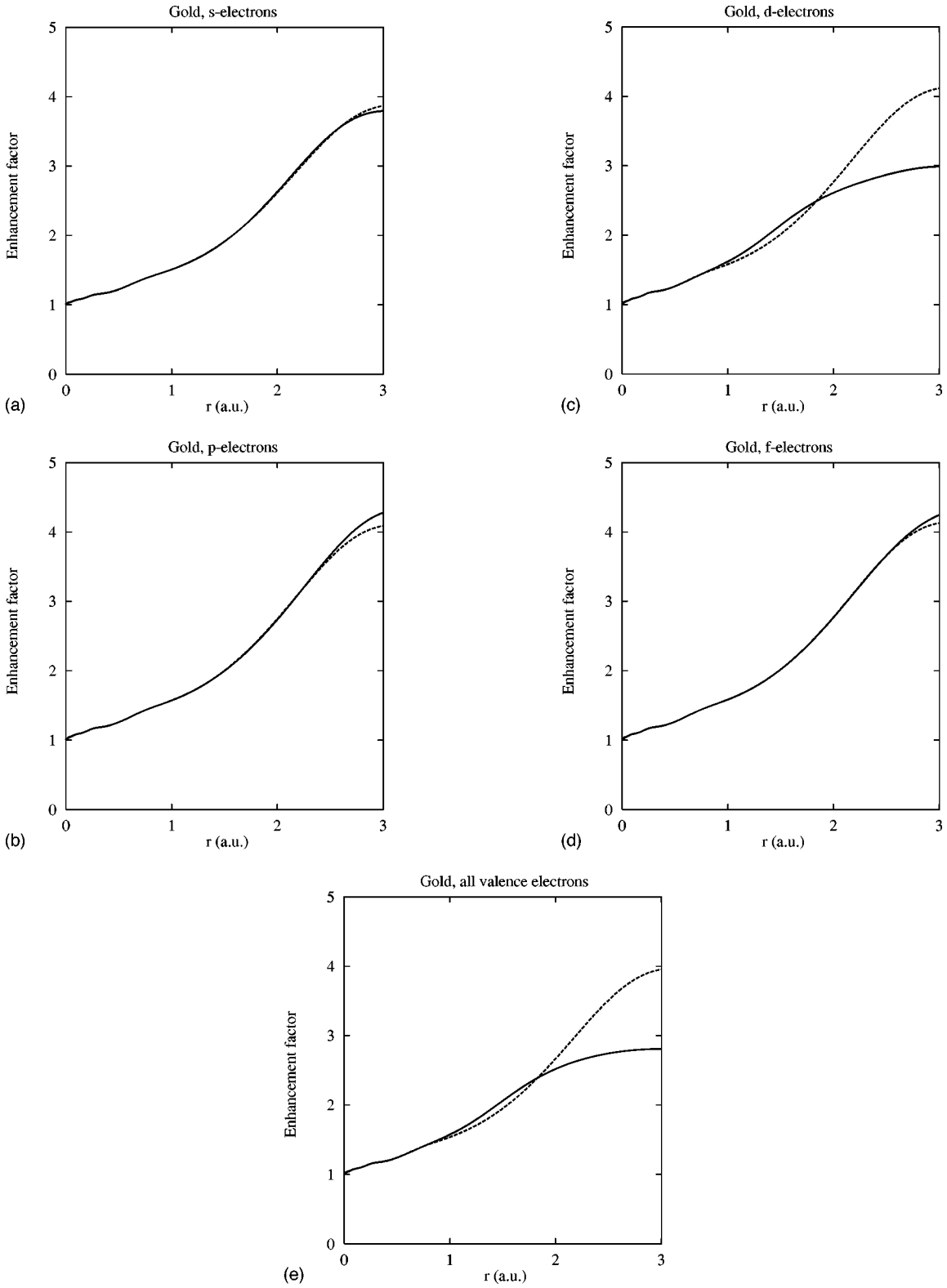

FIG. 3. Enhancement factors for gold, plotted as functions of r, for the *s*-valence electrons (a), *p*-valence electrons (b), *d*-valence electrons (c), *f*-valence electrons (d), and the total number of valence electrons (e). The solid curves represent the WDA results and the dashed curves refer to the LDA calculation.

tron density at the positron site, and are therefore influenced by the shape of the charge density. The WDA enhancement factors, on the other hand, depend on the electron screening charge distribution over the whole coordinate space. This screening charge does not dependent so much on the shape of the charge density (integrated quantities matter now), and therefore should be more reliable even in the vicinity of the ASA sphere boundary.

C. Electron-positron correlation potential and effect of positron distribution on positron annihilation rates

The nonlocal correlation effects, discussed in previous subsections, are also seen in the e-p correlation potentials. In Fig. 4, the WDA e-p correlation potential multiplied by $|\mathbf{r}|$, namely, $rV_{corr}^{WDA}(\mathbf{r})$, calculated according to Eq. (3), is compared with the LDA correlation potential, $rV_{corr}^{LDA}(\mathbf{r})$, respectively, for potassium and gold. Also shown in Fig. 4 are the difference curves, $\Delta V(\mathbf{r})=r[V_{corr}^{WDA}(\mathbf{r})-V_{corr}^{LDA}(\mathbf{r})]$, which reflect nonlocal effects. Note, that for distances close to the nuclei, the WDA potential is more attractive than the LDA potential $[\Delta V(\mathbf{r})<0]$, and that is true for both potassium and gold. This is due to the WDA electron screening charge being shifted towards the nuclei, while the LDA screening charge remains spherically localized around the positron. For $|\mathbf{r}|$'s outside the nuclei, the differences between potassium and gold are much more apparent. In potassium, the WDA dominates over the LDA potential (for $r\geqslant 3.5$ a.u.), suggesting that the valence electrons are more attracted by the positron than predicted by the LDA. For the intermediate distances (for $r\geqslant 2$ a.u.), $\Delta V(\mathbf{r})$ takes positive values, i.e., the WDA potential is weaker than its LDA counterpart. This is a result of the shift of the core part of the screening cloud towards the nuclei, and the valence part towards large $|\mathbf{r}|$'s, where the valence electrons are mostly found. In gold, in the range of large $|\mathbf{r}|$'s (for $r>2$ a.u.), $\Delta V(\mathbf{r})$ is a monotonically increasing positive function, implying that V_{corr}^{LDA} is more attractive than the WDA potential. For the intermediate $|\mathbf{r}|$'s, $\Delta V(\mathbf{r})$ is negative, because the positron interacts mostly with d electrons that dominate in the valence electron density of gold. It further implies that in that region the positron is screened by the valence electrons more than it would follow from the LDA. Hence, the WDA e-p correlation potential is more attractive than the LDA e-p correlation potential. For $|\mathbf{r}|$'s in the vicinity of the ASA sphere boundary, the electron screening cloud in gold is shifted towards the intermediate $|\mathbf{r}|$'s, and the resulting WDA e-p correlation potential becomes weaker than V_{corr}^{LDA}.

The corresponding positron distributions, $|\psi_{+}^{WDA}(\mathbf{r})|^2$ and $|\psi_{+}^{LDA}(\mathbf{r})|^2$, relative to the IPM distribution, are shown in Fig. 5, for both potassium and gold. One can see that, as compared to the IPM, the weights of the WDA and LDA positron distributions are shifted towards the region of small $|\mathbf{r}|$'s. This effect is easy to understand, because the screened positron appears more neutral to the ions. As a result, the e-p correlations increase the overlap of the positron wave function with the core electrons, and hence the corresponding core contribution to the positron annihilation characteristics.

Regarding the nonlocal effects, they differ substantially between potassium and gold, mostly due to the importance of the positron interaction with the d electrons in gold. Since the positron interacts with its screening cloud, it is most likely to be found in regions where the screening cloud is shifted towards. Therefore, it is obvious that, in regions where V_{corr}^{WDA} is stronger than V_{corr}^{LDA}, $|\psi_{+}^{WDA}|^2$ is larger than $|\psi_{+}^{LDA}|^2$, and vice versa.

For potassium, the comparison of the LDA with the WDA shows that the sp-like part of the valence electrons polarization cloud is shifted away from the intermediate $|\mathbf{r}|$'s towards the ASA sphere boundary. Since the positron follows its screening charge, therefore the probability of finding it in the vicinity of the ASA sphere boundary should be higher in the WDA than in the LDA. In gold, the electron screening cloud is mostly due to d electrons, so the WDA screening charge, and hence the positron itself, are pinned more to the range of the intermediate $|\mathbf{r}|$'s, than predicted by the LDA calculations. Consequently, the WDA positron distribution in gold is shifted towards the intermediate $|\mathbf{r}|$'s region, as compared to the LDA. The resulting d-electron contribution to the total annihilation rate, calculated according to Eq. (4) using $\psi_{+}^{WDA}(\mathbf{r})$, should be larger in transition metals than the corresponding quantity calculated using $\psi_{+}^{LDA}(\mathbf{r})$. Finally, note that the effect of nonlocality in the positron distribution is 2 to 4 times larger in gold than in potassium. This result is due to the more localized nature of the valence electrons in gold.

Let us now concentrate on the influence of the positron wave function on the partial annihilation rates. For this we start with the discussion of the IPM results, because they contain unperturbed information on the overlap of the electron and positron wave functions. To facilitate this, we have defined a quantity

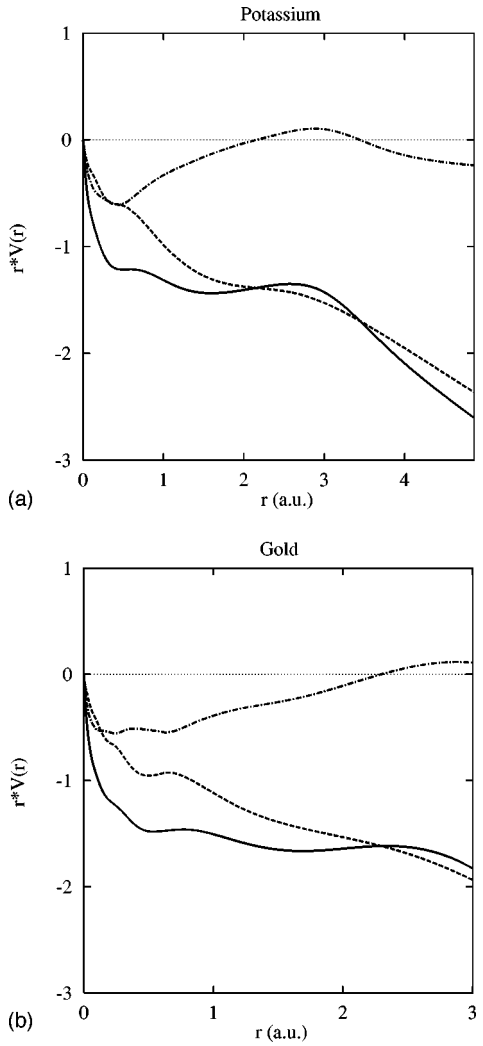

FIG. 4. The positron correlation potentials multiplied by r for potassium (a) and gold (b). The solid lines represent the WDA result, the dashed curves refer to the LDA calculation, and the dash-dotted curves represent their differences.

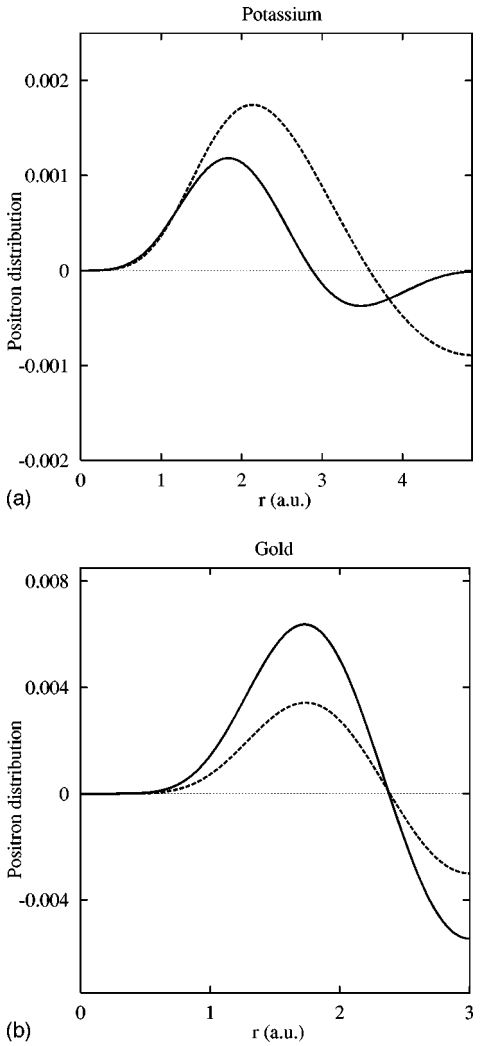

FIG. 5. Positron densities, with respect to the IPM result, multiplied by 4π, plotted as functions of r, and corresponding to the positron correlation potentials of potassium (a) and gold (b). The solid curves represent the WDA result and the dashed curves are due to the LDA.

$$r_t^{LDA(WDA)} = \{\lambda_t^{IPM}(\psi_+^{LDA(WDA)}) - \lambda_t^{IPM}(\psi_+^{IPM})\}/\lambda_t^{IPM}(\psi_+^{IPM}),$$

which reflects the relative changes in λ_t^{IPM} due to different positron wave functions. Again, the subscript t refers to different electrons, while the superscript in ψ_+ refers to the approximation used for the e-p correlation potential and in λ_t to the approximation used for the enhancement factors $\gamma_t(\mathbf{r})$. The quantities r_c^{LDA} and r_c^{WDA} for the core electrons are given in Table I. The first thing to note about r_c^{LDA} and r_c^{WDA} is that they are positive for all these systems. In silicon, calcium, and alkali metals, with the exception of Li, this effect is rather large for the LDA, with r_c^{LDA} of the order of 20%, but it is about 2 to 4 times smaller in the remaining systems. For the WDA, with the exception of K, Rb, and Cs (characterized by rather large cores), r_c^{WDA} is larger than r_c^{LDA}, i.e., the overlap of the WDA positron wave function ψ_+^{WDA}, with the core electrons density, is greater than the overlap for the LDA positron wave function, ψ_+^{LDA}. Except for K, Rb, Cs, Nb, and Mo, the values of r_c^{WDA} are about 1.5 times greater than those of r_c^{LDA}. This implies that the nonlocal effects in the positron wave function are substantially more visible in the WDA core annihilation rates than in their LDA counterparts. Finally, for K, Nb and Mo, the values of r_c^{LDA} and r_c^{WDA} are comparable in magnitude.

Moving on to the valence electrons, one can see in Table II that the s-electron's contribution to the total annihilation rate is hardly affected by the shape of the positron distribution. With the exception of Si, the values of r_s^{LDA} do not exceed 0.5%, and they are in general negative (except for Al, Au, and Si). In comparison with the IPM wave function, the LDA positron wave function is shifted in space from the region preferred by s electrons towards the nuclei, and to those regions where the d electron's distribution has its highest weight. This effect is slightly more pronounced for the WDA positron wave function. The influence of the positron wave function on the p electron contribution to the total annihilation rates is marginally larger than for s electrons. The values of $r_p^{LDA(WDA)}$ are slightly larger than $r_s^{LDA(WDA)}$. With the exception of Si, the values of r_p^{LDA} do not exceed 1.5% and are negative. Also, the values of r_p^{WDA} (which are generally larger than r_p^{LDA}'s) are negative, except for Rb, Cs, and Si. The influence of the shape of the positron wave function on the $d+f$ electron's contribution to the annihilation rate is rather weak for the alkali metals and Al. In the $3d$ transition metals, r_{d+f}^{LDA} is positive and increases from 1.3% in V to 3.9% in Cu, while r_{d+f}^{WDA} is larger and varies from 2% in V to 7.7% in Cu. In the $4d$ and $5d$ transition metals r_{d+f}^{LDA} takes values in the range of 0.7%–4.1%, and r_{d+f}^{WDA} can rise up to 6.3%. In all transition metals r_{d+f}^{WDA} is larger than r_{d+f}^{LDA}, i.e., the nonlocal correlation effects increase the overlap of the positron wave function with the d electrons distribution. For the total number of valence electrons, the values of $r_v^{LDA(WDA)}$ are listed in Table III. For Li, Na, and Al, there is hardly any influence of the positron distribution on the valence annihilation rates. In the remaining systems the values of r_v^{WDA} are 1.5 to 2.5 times larger than those of r_v^{LDA}. In transition metals the values of $r_v^{LDA(WDA)}$ increase with the filling of the d shell and at the same time the differences between r_v^{LDA} and r_v^{WDA} also increase.

Among all these systems, silicon is in a class of its own. The shape of the positron distribution has considerable influence on all the electron contributions to the annihilation rates. Silicon crystallizes in the diamond structure, which is an open structure. To obtain a realistic electronic structure, empty spheres are included in the LMTO-ASA calculation. It is in the empty spheres that the positron distribution has the highest weight (about 75%). The core electrons are associated with the ions, namely, the Si spheres in our calculations. Therefore, already small changes in the positron potential cause substantial changes in the positron overlap with the core electrons distribution. In Si the values of r_c^{LDA} and r_c^{WDA} are as large as 27% and 48%, respectively. Note that, applying the WDA e-p correlation potential, V_{corr}^{WDA} shifts the weight of the positron distribution from empty to Si spheres, as compared with the LDA and IPM. The valence electrons in Si, which have an sp-like character, have also their weight associated with the Si spheres. Inclusion of the e-p correlation potential in the positron Schrödinger equation has the

largest effect on the p part of the positron annihilation rate: the corresponding values of r_p are as large as 7.2% for the LDA, and 10.7% for WDA. For s electrons the relevant quantities have slightly smaller values, namely 5.2% and 7.8%, respectively, for the LDA and WDA.

D. Effect of electron-positron correlations on positron annihilation rates

The e-p interaction affects both the positron distribution and the electron density at the positron position. To discuss the effect of the enhancement of the electron density at the positron position on the positron annihilation rates, it is convenient to define, following Refs. 5, 17, 18, 20, and 26, the average enhancement factors $\Gamma_t^{LDA}=\lambda_t^{LDA}(\psi_+^{LDA})/\lambda_t^{IPM}(\psi_+^{LDA})$ and $\Gamma_t^{WDA}=\lambda_t^{WDA}(\psi_+^{WDA})/\lambda_t^{IPM}(\psi_+^{WDA})$, respectively, for the LDA and WDA. These average enhancement factors Γ_t can be interpreted as the enhancement factors $\gamma_t(\mathbf{r})$ in the region, where the overlap of the various electron distributions with the positron distribution is largest. Again, the superscript of λ refers to the approximation used for the e-p enhancement factors, $\gamma_t(\mathbf{r})$, and the superscript in ψ_+ stands for the approximation employed for the e-p correlation potential V_{corr} in the positron Schrödinger equation.

The quantities $\Gamma_t^{LDA(WDA)}$ contain information on the e-p enhancement factors $\gamma_t^{LDA(WDA)}(\mathbf{r})$, weighted by the positron distribution, $|\psi_+^{LDA(WDA)}(\mathbf{r})|^2$. However, to study how the e-p correlations affect the positron annihilation rates, one should rather compare the LDA with the WDA quantities, in reference to the IPM quantity, in case where both the enhancement factors and the positron wave functions refer to the same approximation. In fact, it is the quantities $(1+r_t^{LDA})\Gamma_t^{LDA}$ and $(1+r_t^{WDA})\Gamma_t^{WDA}$ that provide the full information on the changes in the corresponding annihilation rates $\lambda_t^{LDA(WDA)}$, due to both the e-p enhancement factor and the positron distribution. The quantities r_t have already been discussed and the remaining ingredients of $(1+r_t^{LDA})\Gamma_t^{LDA}$, namely, Γ_t, are given in Table I for the core electrons, and in Tables II and III for the valence electrons, decomposed into various angular momentum channels and the total number of valence electrons, respectively.

In all the systems we studied, the quantities Γ_c for the core electrons are larger than unity, indicating some deviation from the IPM: the LDA values of Γ_c are larger than 1.7, and the WDA values are larger than 1.54. Moreover, except for Li, Al, and Si, the WDA e-p enhancement factors are generally considerably smaller than the LDA values. The reason is that, as seen in Fig. 1, in the regions where the positron can be found with the highest probability, the WDA core electron's enhancement factor, $\gamma_c^{WDA}(\mathbf{r})$, is substantially smaller than the LDA core electron's enhancement factor, $\gamma_c^{LDA}(\mathbf{r})$. In transition metals, the core electrons are distributed over the high-density region. Therefore, the values of $\Gamma_c^{LDA(WDA)}$ are not too large (smaller than 2.3). As a consequence, the core electron's enhancement factors of the alkali metals are greater than the ones in the transition metals. It may be of interest that the values of Γ_c obtained within GGA by Alatalo *et al.*[17] for Al, Si, Ni, and Cu are very similar to the Γ_c^{WDA} of the present calculation. Moreover, the values of Γ_c^{LDA}, as calculated in the present paper using the approach of Daniuk *et al.*,[5] are also very close to the GGA result. However, it is not the case for the values of Γ_c^{LDA}, as reported by Alatalo *et al.*,[17] which are substantially larger than the WDA result. This implies a crucial dependence of the LDA result on the approach to the core electrons enhancement factors.

The nonlocal effects in the positron distribution, expressed in terms of the quantities r_c (Table I), which are generally greater for the WDA than for the LDA, do not compensate for the strong reduction of the WDA core enhancement factors Γ_c^{WDA}, with respect to the LDA values, Γ_c^{LDA}. As a result, with the exception of Si and Li, the full nonlocal e-p correlation effects reduce the core contribution to the total annihilation rates. It seems that Li is a special case since, surprisingly, the $1s$ core electrons behave very much like the valence $2s$ electrons. In general, the core electrons contributions to the total annihilation rates are not negligible: the average contribution of λ_c is of the order of 5–15%. In silicon, the values of Γ_c^{WDA} and Γ_c^{LDA} are similar in magnitude, while the overlap of the WDA positron wave function ψ_+^{WDA} with the wave function of the core electrons is about 20% greater than for the LDA positron wave function ψ_+^{LDA}. Therefore, the nonlocal e-p correlation effects increase the values of the core annihilation rates, as compared to the LDA. In Si the core electrons contribution to the total annihilation rate is, however, very small, not exceeding 3%.

For the valence electrons, the average enhancement factors $\Gamma_{s,p,d+f}^{LDA(WDA)}$ for different angular momentum channels, are given in Table II. In Table III we give the results for the total number of valence electrons. The $\Gamma_{s(p)}^{WDA}$'s and $\Gamma_{s(p)}^{LDA}$'s are very similar, with a trend of slightly larger $\Gamma_{s(p)}^{WDA}$'s. In contrast, in silicon the values of $\Gamma_{s(p)}^{WDA}$ are considerably lower than their LDA counterparts. The effect of nonlocality in the enhancement factors is to dampen the influence of the positron wave function [represented by the values of $r_{s(p)}^{LDA}$ and $r_{s(p)}^{WDA}$]. As a result, with the exception of Si, the annihilation rates, $\lambda_{s(p)}^{WDA}$ (see Table IV) are a little larger than the LDA values, $\lambda_{s(p)}^{LDA}$. The values of the average enhancement factors Γ_d^{WDA} in the alkali metals are greater than their LDA counterparts. The effect of the e-p enhancement factors is reduced by the influence of the positron wave function, and there is no significant difference between the LDA and WDA values of λ_d in simple metals. Contrary to the alkali metals, the values of Γ_{d+f}^{WDA} in transition metals are considerably smaller than Γ_{d+f}^{LDA}'s. As shown in Fig. 3, for transition metals, in those regions where the positron wave function has a substantial weight, the WDA e-p enhancement factors, $\gamma_d^{WDA}(\mathbf{r})$ are considerably smaller than the LDA enhancement factors $\gamma_d^{LDA}(\mathbf{r})$. As a result, the corresponding average enhancement factors Γ_d^{WDA} are smaller than the LDA values Γ_d^{LDA}. In the $3d$ and $4d$ metals, the values of $\Gamma_d^{LDA(WDA)}$ decrease slightly with increasing the atomic numbers. The strong reduction of the WDA enhancement factor, with respect to the LDA value, cannot be compensated by a rather small increase of r_{d+f}^{WDA}, as compared to r_{d+f}^{LDA}. Therefore, applying WDA considerably reduces the values of λ_{d+f}'s in the d-electron metals, with respect to the corresponding LDA values.

TABLE V. Positron lifetimes calculated according to Eq. (4) using four different parametrizations of $\gamma^h(n_0)$, namely, BN, AP, SL, and RS. The superscripts of τ specify the approximation used for the e-p enhancement factors $\gamma_t(\mathbf{r})$, and the approximation used for the e-p correlation potential V_{corr} used in the positron Schrödinger equation. The lifetime τ_1^{LDA} has been calculated in the state-independent approach using the LDA formula. Also shown is the GGA calculation and the experimental lifetimes, where available.

	BN			AP			SL		RS		GGA	
(1) Element	(2) τ^{LDA}	(3) τ_1^{LDA}	(4) τ^{WDA}	(5) τ^{LDA}	(6) τ_1^{LDA}	(7) τ^{WDA}	(8) τ^{LDA}	(9) τ^{WDA}	(10) τ^{LDA}	(11) τ^{WDA}	(12)	(13) τ_{exp}
Alkali metals												
Li	306.4	300.4	299.4	267.5	260.3	255.1	284.4	250.4	302.9	279.0		291
Na	339.5	328.1	334.7	305.4	290.9		322.7		337.5	337.2	329	338
K	383.2	366.9	395.5	354.6	330.9	373.9	372.7	395.4	392.5	422.1	392	397
Rb	395.9	376.6	425.2	370.5	342.1		388.3		409.1	467.8		406
Cs	413.0	389.3	452.8	391.5	357.2		409.2		430.3	492.8		418
Polyvalent metals												
Ca	274.5	273.4	384.2	238.5	237.2	338.8	254.3	380.2	247.8	390.1		
Al	165.9	163.4	163.3	147.2	144.8		155.4		161.3	157.7	153	163
$3d$ transition metals												
V	118.4	114.0	129.8	109.2	131.1		113.8		111.5	118.7	119	130
Cr	102.5	98.9	112.9	95.4	91.7		99.2		99.5	105.9		120
Mn	105.1	101.9	118.0	97.5	94.3	112.1	101.5	106.1	100.8	107.9		
Fe	102.1	99.3	111.8	94.9	92.1		98.8		98.2	105.8	108	106
Ni	97.3	95.1	112.1	90.7	88.6	109.1	94.4	102.4	93.4	101.2	107	110
Cu	106.6	104.6	122.8	98.6	96.8	122.3	102.9	116.1	104.3	113.4	118	110
$4d$ transition metals												
Nb	124.3	119.6	129.4	114.5	109.0		119.3		117.9	126.7	122	119
Mo	105.5	101.7	109.7	98.1	94.0		102.0		104.0	111.1	112	103
Pd	103.9	101.4	114.9	96.5	94.1	113.4	100.5	112.3	102.4	111.5	114	96
Ag	121.5	119.1	139.4	111.5	109.2	136.4	116.6	131.3	123.2	134.9		131
$5d$ transition metals												
Pt	95.1	93.0	103.1	88.7	86.7		92.4	102.6	93.8	100.5	101	99
Au	108.0	106.0	120.3	99.8	97.9	117.2	104.2	111.5	107.8	115.5		117
Semiconductors												
Si	211.7	210.5	217.0	186.4	185.4		197.7		204.3	216.7	210	219
Mean error for 12 elements												
	6.39	8.93	5.68	17.18	19.82		10.58		6.98	7.50	7.42	

The annihilation rates for the total number of valence electrons, λ_v^{LDA} and λ_v^{WDA} (see Table III), reflect features of the specific angular momentum channels. In alkali metals, Al and Si, valence electrons and the corresponding annihilation rates have the sp character. As seen in Table IV, in the alkali metals, the s electron's contribution to the total annihilation rate is slightly larger than the contribution due to the p electron's, while in Al and Si, the values of λ_p are greater than those of λ_s. These features are common for the LDA and WDA. The corresponding enhancement factors $\Gamma_v^{LDA(WDA)}$ fall in between the values of $\Gamma_s^{LDA(WDA)}$ and $\Gamma_p^{LDA(WDA)}$. As a result, in alkali metals and Al, the nonlocal e-p correlation effects increase the valence electron's annihilation rate, λ_v^{WDA}, as compared with the LDA annihilation rate, while in Si the annihilation rate λ_v^{WDA} is smaller than λ_v^{LDA}. Since the valence electrons in the alkali metals are jelliumlike, it is not surprising that both $\Gamma_{s,p,d+f}^{LDA(WDA)}$ and $\Gamma_v^{LDA(WDA)}$ are increasing functions of the lattice constant. In transition metals and Ca, the valence electrons density is mainly d-like. The d electrons contribution, λ_d, dominates in the valence electrons annihilation rates. Also, the quantities $\Gamma_v^{LDA(WDA)}$ reflect the d-like character of the valence electrons in these systems. Therefore, the WDA also reduces the average valence enhancement factors, Γ_v^{WDA}, in comparison with the LDA. As a result, the nonlocal effects reduce λ_v^{WDA}, as compared to λ_v^{LDA}, and the valence electron's annihilation rates, λ_v^{WDA}, are considerably smaller than the LDA values.

E. Positron lifetimes

In this subsection we concentrate on the calculated positron lifetimes, obtained as an inverse of the positron annihi-

lation rates, and compare them in Table V with the measured values,[25] and with the GGA calculation of Ref. 26. The positron lifetimes τ_1, calculated in the state-independent approach, are also given for comparison. In the last row of Table V, we give the mean error between the calculated and experimental positron lifetimes, namely, $error = (1/n)\Sigma_i|\tau_i^{cal} - \tau_i^{exp}|$, averaged only over these systems that are listed in column (12). These errors provide a quantitative assessment of the WDA and LDA results with respect to the experimental data.

Note that the LDA lifetimes, calculated with the AP parametrization of the enhancement factors $\gamma^h(n_0)$, are in general shorter than the lifetimes corresponding to the remaining parametrizations. In transition metals, characterized by rather high electron densities, the SL and RS values of τ^{LDA} are very close to each other, but smaller than the corresponding BN lifetimes. In K, Rb, and Cs, where the electron density in the interstitial region is relatively low, the RS parametrization of $\gamma^h(n_0)$ leads to larger lifetimes, τ^{LDA}, than those obtained with the remaining parametrizations.

Neglecting the state selectivity of the enhancement factors $\gamma_t(\mathbf{r})$ leads to an increase of the total annihilation rates. Therefore, the values of τ_1^{LDA} are in general smaller than the values of τ^{LDA}. The reason seems rather obvious: the core contribution to τ_1, calculated in the state-independent approach, is greater than the core contribution to τ, calculated using the LDA approach of Daniuk *et al.*,[5,6] because the corresponding local enhancement factors, $\gamma^h[n(\mathbf{r})]$, for the core electrons are greater than $\epsilon[0,n(\mathbf{r})]$.

With the exception of Al, Li, and Na, the WDA gives longer positron lifetimes than the LDA. In the alkali metals, this is mainly due to the positron annihilation with the core electrons. In transition metals, the WDA *d* electrons contribution to the annihilation rates is considerably smaller than the LDA contribution. In Al, Li, Na, and K, the WDA, combined with the BN parametrization of the enhancement factors $\gamma^h(n_0)$, provides the best agreement between the calculation and experiment. When the state-selective (RS) enhancement factors are used in Eq. (4), the experimental lifetimes fall in between the LDA and WDA values. The same happens in Rb and Cs when the BN parametrization is used in Eq. (4). Both, the LDA and WDA lifetimes, calculated with the use of the RS parametrization, are longer than the experimental values τ_{exp}. It may be of interest here that for low electron densities, occurring in the interstitial regions of K, Rb, and Cs, the RS values of the enhancement factors $\gamma^h(n_0)$ are too small in comparison with other jellium results. In transition metals, the WDA improves the agreement between theory and experiment. In V, Cr, Ni, Mo, and Si, the BN parametrization leads to the best agreement with experiment, and in Fe, Cu, Nb, Pd, Ag, Pt, and Au, the RS parametrization provides better results. Note, that in Na, Nb, Mo, and Pd, the positron lifetimes, calculated within the LDA, combined with the RS parametrization, are closer to experiment than the WDA lifetimes. Also, in Cs the LDA combined with the BN parametrization provides best agreement with the experimental data owing to the *t* selectivity of the correlation functions γ_t, which plays an important role. Note that also the LDA results for these systems are in better agreement with the experiment than the GGA values.[26] When analyzing the mean errors quoted in Table V, one can see that the WDA combined with the BN parametrization gives the best results. Moreover, the LDA results, with the approach of Daniuk *et al.*[5] regarding the core electrons enhancement factors, are also in better agreement with experiment than the GGA results. As far as other parametrizations are concerned, the mean error for the RS parametrization is rather large due to an unsatisfactory result for potassium, caused by rather low electron density. Removing potassium from the summation when evaluating the mean error would reduce its value from 7.5 to 5.9 psec.

TABLE VI. Positron lifetimes in silicon calculated for different approximations according to Eq. (4), using the RS and BN parametrizations of $\gamma_t^h(n_0)$. The superscripts of τ specify the approximation used for the e-p enhancement factors, $\gamma_t(\mathbf{r})$. The lifetimes τ_1^{LDA} have been calculated in the state-independent approach, according to the LDA formula for λ_1.

	BN			RS	
(1)	(2) τ^{LDA}	(3) τ_1^{LDA}	(4) τ^{WDA}	(5) τ^{LDA}	(6) τ^{WDA}
ψ_+^{IPM}	219.3		229.4	211.6	231.8
ψ_+^{LDA}	211.7	210.5	220.0	204.3	221.3
ψ_+^{WDA}	209.2		217.0	200.5	216.1

Finally, in Table VI we present the positron lifetimes for Si, calculated for all different approximations concerning the positron wave function and the e-p correlations. We have used both the BN and RS parametrizations as the input correlation functions $\gamma_t^h(n_0)$. The BN parametrization gives best agreement with the experimental value of 219 ± 2 psec in two cases. First, within the WDA with the WDA positron wave function, namely, for $\tau^{WDA}(\psi_+^{WDA})$, and second, within the LDA with the IPM positron wave function, namely, for $\tau^{LDA}(\psi_+^{IPM})$. In the second case, the LDA values of the enhancement factors $\gamma_t(\mathbf{r})$ have been used and the e-p correlation potential V_{corr} has been neglected in the positron Schrödinger equation. Although giving better agreement with experiment, the second approach violates the Feynmann's theorem relating the e-p correlation potential to the electron distribution of the screening cloud surrounding positron [see Eq. (3)]. For the RS parametrization of the enhancement factors $\gamma^h(n_0)$, it is the WDA that leads to the best agreement with experiment.

Comparing the WDA with the LDA, we find, as expected, that for nearly free-electron-like systems, both approaches give similar annihilation rates. However, nonlocal effects are very important for the core electrons contribution to the total annihilation rates. They are equally important for the *d* electrons in transition metals. These nonlocal effects are included in the WDA in an average manner, through distributing the partial electron densities over the whole WS cell. Also, the state selectivity of the e-p correlation functions is of importance for calculations of the positron annihilation rates in solids. Moreover, the BN parametrization of the enhancement factors $\gamma^h(n_0)$ appears to be the best parametrization for metals with low electron densities in the interstitial region. In Si, the WDA provides a more reliable description of the e-p correlations than the LDA. Therefore, this gives us confidence to apply the WDA in the calculation of e-p momentum distributions, especially for Si. It is with Si and

transition metals in mind, that the present implementation has been undertaken in the first place.

IV. CONCLUSIONS

Summarizing the results of this paper, it is fair to say that the WDA gives a substantially different picture of the e-p correlations in solids than the LDA. What the LDA and WDA have in common is that different electrons give different contributions to the screening cloud surrounding positron. The essential difference between the two approximations is in the shape of the screening charge distribution that is spherically symmetric in the LDA, but in the WDA it is asymmetric, through sampling the electron distribution in the whole ASA sphere, and is strongly dependent on the type of electrons considered. For a given type of electrons, the WDA contribution to the screening charge distribution is asymmetric towards regions in space preferred by these electrons. As a result, the nonlocal effects slightly increase the enhancement factors of the core electrons for small positron distances from the nuclei, but reduce them considerably for large $|\mathbf{r}|$'s, in the vicinity of the ASA sphere boundary. A similar effect is observed for the d electron's enhancement factors in gold, which are larger than the LDA enhancement factors, for $|\mathbf{r}|$'s of relevance to d electrons. However, for large $|\mathbf{r}|$'s, namely, in the vicinity of the ASA sphere boundary, the WDA enhancement factors are considerably smaller than the LDA enhancement factors $\gamma_d^{LDA}(\mathbf{r})$. As expected, the nonlocal effects are not of much significance for nearly free electrons, since the WDA enhancement factors are rather LDA-like. The WDA e-p enhancement factors are less dependent on the positron position than it is observed within the LDA. The state selectivity of the input jellium enhancement factors is exactly reproduced within the LDA, while the WDA always provides the state-selective enhancement factors, except for the case of the constant electron density of the host material. Comparing the present theory and the GGA approach,[26] one should note that the WDA enhancement factors for nearly free electrons differ appreciably from the corresponding quantities for the localized core and d electrons, while within GGA (Ref. 26) all types of electrons scatter on the positron at the same rate. Therefore, although the WDA and GGA (Refs. 17 and 26) provide similar patterns in the enhancement factors for the core electrons, as compared with the LDA, nevertheless considerable differences are observed between the WDA and GGA enhancement factors for valence electrons, both in simple and transition metals.

The nonlocal effects are even more pronounced in the e-p correlation potential, both in simple metals like potassium, and in transition metals, represented here by gold. As a result, the WDA alters the e-p correlation energy and positron distribution in solids. The WDA results are strongly dependent on the degree of localization of the valence electrons in a given system. In particular, in transition metals, in variance to the LDA, in the WDA the positron is found with higher probability in the region where the localized d electrons are found. In simple metals the positron is expected to be found most likely close to the ASA sphere boundary.

The present calculations show that the shape of the positron wave function is of considerable significance for the core contribution to the annihilation rates, which confirms the results of earlier calculations.[5] It is also of importance for the partial annihilation rates due to the localized d electrons in transition metals. However, the shape of the positron wave function seems to be of no significance for the nearly free sp-like valence electrons contribution to the total annihilation rates. Our results also suggest that the state selectivity of the e-p correlation functions is of vital importance in calculations of the positron annihilation characteristics in solids. In the many systems studied in this paper, the WDA, combined with the BN parametrization of the jellium correlation functions, gives a very good agreement with the available experimental data. Especially, for silicon the WDA seems to be necessary for obtaining realistic results. However, it is not always true that the WDA results agree better with experiments than the LDA calculations. In several systems, the measured lifetimes lie inbetween the LDA and WDA values, while in others the LDA lifetimes are in better agreement with experiments. Note that for nearly free sp-like valence electrons, both the LDA and WDA lead to similar results. Nevertheless, it seems that for the localized d electrons in transition metals as well as for core electrons, the nonlocality of the e-p correlations should be taken into account in calculations of the positron annihilation characteristics. Although the WDA should not be treated as the alternative for the full many-body calculations of the e-p correlations, however, one can at least say that by considering the important nonlocal effects, this approach leads to rather encouraging results. We think that it will be vital for the e-p momentum distributions, which we are currently implementing, and in particular in Si.

ACKNOWLEDGMENT

We are grateful to the Royal Society for partial financial support of this work.

APPENDIX

Here we give some additional technical details on calculating the effective densities $\tilde{n}_t(\mathbf{r}_p)$. The LMTO-ASA provides the charge densities $n_t(\mathbf{r}_e)$ in the Wigner-Seitz (WS) sphere only. However, the integrations in Eqs. (2) and (5) run over the whole space Ω. Moreover, the effective densities $n_t^*(\mathbf{r}_e)$, as the normal densities $n_t(\mathbf{r}_e)$, have to be spherically symmetric inside the WS sphere. Therefore, in the present paper we have implemented two different methods of dealing with the densities. The first method is based on the values of $n_t(\mathbf{r}_e)$ in the whole coordinate space. For this the spherical average of the densities, $n_t(\mathbf{r}_e)$, for $|\mathbf{r}_e| \geqslant S_0$, has been evaluated in the form

$$n_t(|\mathbf{r}_e|) = \sum_{|\mathbf{R}_i - \mathbf{r}_e| \leqslant S_i} \frac{2}{R_i} \int_{|R_i - r_e|}^{S_i} x n_t(x)\,dx \times \left\{ \sum_{|\mathbf{R}_i - \mathbf{r}_e| \leqslant S_i} \frac{1}{R_i} [S_i^2 - |R_i - r_e|^2] \right\}^{-1},$$

where $\mathbf{R}_i$ are the lattice vectors ($\mathbf{R}_0 = \mathbf{0}$), and S_i are the radii of the WS spheres centered on $\mathbf{R}_i$'s. In the second method, the WS cells have been replaced by the WS spheres and the integral in Eq. (5), for $\mathbf{r}_p$ inside the spheres, has been calculated according to the formula

$$\int_{\Omega} n_t(\mathbf{r}_e) e^{-a[\tilde{n}_t(\mathbf{r}_p)]|\mathbf{r}_e-\mathbf{r}_p|} d\mathbf{r}_e$$

$$\cong \sum_{\mathbf{R}_i} \int_{|\mathbf{r}|\leqslant S_i} n_t(|\mathbf{r}|) e^{-a[\tilde{n}_t(|\mathbf{r}_p|)]|\mathbf{r}+(\mathbf{R}_i-\mathbf{r}_p)|} d\mathbf{r},$$

where $|\mathbf{R}_i-\mathbf{r}_p|$ has been approximated by the spherical average of the form

$$\langle|\mathbf{R}_i-\mathbf{r}_p|\rangle = \frac{1}{2}\int_{-1}^{1} |\mathbf{R}_i-\mathbf{r}_p| d\,\cos(\Theta),$$

Θ being the angle between $\mathbf{R}_i$ and $\mathbf{r}_p$. The densities $\tilde{n}_t(\mathbf{r}_p)$, obtained using both methods have turned out to be in a very good agreement with each other (within 0.5%).

*Electronic address: Z.Szotek@dl.ac.uk

†Electronic address: W.M.Temmerman@dl.ac.uk

[1] For a review, see, e.g., R. N. West, *Positron Studies of Condensed Matter* (Taylor and Francis, London, 1974); S. Berko, in *Positron Solid State Physics*, edited by W. Brandt and A. Dupasquier (North-Holland, Amsterdam, 1983), p. 64; M. J. Puska and R. M. Nieminen, Rev. Mod. Phys. **66**, 841 (1994).

[2] For a review, see, e.g., H. Stachowiak and A. Rubaszek, in *Positrons at Metallic Surface*, edited by A. Ishii (Trans. Tech. Co., Aedermannsdorf, 1993), p. 7.

[3] J. P. Carbotte, in Ref. 1, p. 32; H. Sormann and W. Puff, in *Positron Annihilation*, edited by P. C. Jain, R. M. Singru, and K. P. Gopinathan (World Scientific, Singapore, 1995), p. 161; H. Sormann, Phys. Rev. B **54**, 4558 (1996).

[4] S. Daniuk, G. Kontrym-Sznajd, A. Rubaszek, H. Stachowiak, J. Mayers, P. A. Walters, and R. N. West, J. Phys. F **17**, 1365 (1987).

[5] S. Daniuk, M. Šob, and A. Rubaszek, Phys. Rev. B **43**, 2580 (1991).

[6] S. Daniuk, G. Kontrym-Sznajd, J. Majsnerowski, M. Šob, and H. Stachowiak, J. Phys.: Condens. Matter **1**, 632 (1989).

[7] B. Chakraborty, Phys. Rev. B **24**, 7423 (1981); in *Positron Annihilation*, edited by P. G. Coleman, S. C. Sharma, and L. M. Diana (North-Holland, Amsterdam, 1982), p. 207.

[8] M. Šob, J. Phys. F **12**, 571 (1982); **15**, 1685 (1985); O. Johnson, Phys. Status Solidi B **99**, 745 (1980).

[9] G. Kontrym-Sznajd and A. Rubaszek, Phys. Rev. B **47**, 6950 (1993); **47**, 6960 (1993).

[10] P. E. Mijnarends and R. M. Singru, Phys. Rev. B **19**, 6038 (1979); M. Šob, J. Phys. F **15**, 1685 (1985); A. K. Singh, A. A. Manuel, T. Jarlborg, Y. Mathys, E. Walker, and M. J. Peter, Helv. Phys. Acta **59**, 410 (1986).

[11] S. M. Kim and A. T. Stewart, Phys. Rev. B **11**, 2490 (1975); T. Hyodo, T. McMullen, and A. T. Stewart, in *Positron Annihilation*, edited by P. G. Coleman, S. C. Charma, and L. M. Diana (North-Holland, Amsterdam, 1982), p. 201; P. Kubica and A. T. Stewart, Phys. Rev. Lett. **34**, 852 (1975).

[12] T. Jarlborg and A. K. Singh, Phys. Rev. B **36**, 4660 (1987); T. Jarlborg, E. Walker, A. A. Manuel, and M. J. Peter, *ibid.* **43**, 14 532 (1991).

[13] R. M. Nieminen, in Ref. 1; E. Boroński and R. M. Nieminen, Phys. Rev. B **34**, 3820 (1986).

[14] R. M. Nieminen and M. J. Puska, Phys. Rev. Lett. **50**, 281 (1983); R. M. Nieminen, M. J. Puska, and M. Manninen, *ibid.* **53**, 1298 (1984); M. J. Puska and R. M. Nieminen, J. Phys. F **13**, 2695 (1983).

[15] A. Rubaszek, Phys. Rev. B **44**, 10 857 (1991); A. Rubaszek, A. Kiejna, and S. Daniuk, J. Phys.: Condens. Matter **5**, 8195 (1993).

[16] K. O. Jensen and A. B. Walker, J. Phys. F **18**, L277 (1988).

[17] M. Alatalo, B. Barbiellini, M. Hakala, H. Kauppinen, T. Korhonen, M. J. Puska, K. Saarinen, P. Hautojärvi, and R. M. Nieminen, Phys. Rev. B **51**, 4176 (1995); M. Alatalo, H. Kauppinen, K. Saarinen, M. J. Puska, J. Mäkinen, P. Hautojärvi, and R. M. Nieminen, *ibid.* Phys. Rev. B **54**, 2397 (1996).

[18] K. O. Jensen, J. Phys.: Condens. Matter **1**, 10 595 (1989).

[19] P. A. Sterne and J. H. Kaiser, Phys. Rev. B **43**, 13 892 (1991).

[20] M. J. Puska, J. Phys.: Condens. Matter **3**, 3455 (1991); F. Plazaola, A. P. Seitsonen, and M. J. Puska, *ibid.* **6**, 8809 (1994).

[21] B. Barbiellini, P. Genoud, and T. Jarlborg, J. Phys.: Condens. Matter **3**, 7631 (1991).

[22] S. Kahana, Phys. Rev. **129**, 1622 (1963); W. Brandt and J. Reinheimer, Phys. Lett. **35A**, 109 (1971); J. Arponen and E. Pajanne, J. Phys. C **12**, 3013 (1979), function $\gamma^h(n_0)$ was parametrized by B. Barbiellini, M. J. Puska, T. Torsti, and R. M. Nieminen (Ref. 26) and $V_{corr}(n_0)$ was parametrized by Boroński and Nieminen (Ref. 13); J. Arponen and E. Pajanne, J. Phys. F **9**, 2359 (1979), provide momentum-dependent correlation functions $\epsilon[(E/E_F),n_0]$; A. Kallio, P. Pietiläinen, and L. Lantto, Phys. Scr. **25**, 943 (1982), function $\gamma^h(n_0)$ was parametrized by Boroński and Nieminen (Ref. 13); H. Stachowiak, Phys. Rev. B **41**, 12 522 (1990), function $\gamma^h(n_0)$ and enhancement factors $\epsilon[(E/E_F),n_0]$ were parametrized by H. Stachowiak and J. Lach, *ibid.* **48**, 9828 (1993).

[23] A. Rubaszek and H. Stachowiak, Phys. Status Solidi B **124**, 159 (1984); Phys. Rev. B **38**, 3846 (1988); A. Rubaszek, H. Stachowiak, E. Boroński, and Z. Szotek, *ibid.* **30**, 2490 (1984), provide momentum-dependent correlation functions $\epsilon[(E/E_F),n_0]$.

[24] A. H. Weiss, R. Mayer, M. Jibaly, C. Lei, D. Mehl, and K. G. Lynn, Phys. Rev. Lett. **61**, 2245 (1988); K. O. Jensen and A. H. Weiss, Phys. Rev. B **41**, 3928 (1990); L. Oberli, A. A. Manuel, R. Sachot, P. Descout, and M. J. Peter, *ibid.* **31**, 6104 (1985).

[25] A. Seeger, F. Banhart, and W. Brauer, in *Positron Annihilation*, edited by L. Dorikens-Vanpraet, M. Dorikens, and D. Segers (World Scientific, Singapore, 1989), p. 275.

[26] B. Barbiellini, M. J. Puska, T. Torsti, and R. M. Nieminen, Phys. Rev. B **51**, 7341 (1995); B. Barbiellini, M. J. Puska, T. Korhonen, A. Harju, T. Torsti, and R. M. Nieminen, Phys. Rev. B **53**, 16 201 (1996).

[27] B. Barbiellini, M. Hakala, M. J. Puska, and R. M. Nieminen, Phys. Rev. B **56**, 7136 (1997).

[28] O. Gunnarsson, M. Jonson, and B. I. Lundqvist, Phys. Rev. B **20**, 3136 (1979); R. O. Jones and O. Gunnarsson, Rev. Mod. Phys. **61**, 689 (1989).

[29] P. Hohenberg and W. Kohn, Phys. Rev. **136**, B364 (1964); W. Kohn and L. J. Sham, *ibid.* **140**, A133 (1965).

[30] C. H. Hodges and M. J. Stott, Phys. Rev. B **7**, 73 (1973).

[31] The exponential form of Δn neglects the Friedel oscillations in the screening charge density. This problem is addressed by E. Boroński and H. Stachowiak, Phys. Rev. B **57,** 6215 (1998).

[32] O. K. Andersen, Phys. Rev. B **12**, 3060 (1975); W. R. L. Lambrecht and O. K. Andersen, *ibid.* **34**, 2439 (1986).